

UNCLASSIFIED

AD NUMBER

AD809558

LIMITATION CHANGES

TO:

Approved for public release; distribution is unlimited.

FROM:

Distribution authorized to U.S. Gov't. agencies and their contractors; Critical Technology; NOV 1966. Other requests shall be referred to Air Force Materials Laboratory, Wright-Patterson AFB, 45433. This document contains export-controlled technical data.

AUTHORITY

USAFSC ltr, 26 May 1972

THIS PAGE IS UNCLASSIFIED

Not Dup

1/12/68

①

AFML-TR-67-21

AD No. 809558

DUPLICATE FILE COPY

FINAL REPORT ON THE DEVELOPMENT OF HIGH PERFORMANCE POROUS TUNGSTEN IONIZERS

NOVEMBER 1966

Metallurgical Processing Branch
Manufacturing Technology Division
Air Force Material Laboratory
Research and Technology Division
Air Force Systems Command
United States Air Force
Wright-Patterson Air Force Base, Ohio

This document is subject to special export controls and each transmittal to foreign governments or foreign nationals may be made only with prior approval of the Manufacturing Technology Division.

(Prepared under Contract AF 33(615)-3817 by

TRW
SYSTEMS GROUP

M. E. Kirkpatrick and R. A. Mendelson, Authors)

DDC
REC
MAR 24 1967
R
B

ACQUISITION BY	
CPDR	PRIME SERVICE <input type="checkbox"/>
NSC	SWT SERVICE <input type="checkbox"/>
UNCLASSIFIED	<input type="checkbox"/>
JUSTIFICATION	
BY	
RESTRICTION/AVAILABILITY CODES	
DIST.	AVAIL. and/or SPECIFIC
2	

NOTICES

When Government drawings, specifications, or other data are used for any purpose other than in connection with a definitely related Government procurement operation, the United States Government thereby incurs no responsibility nor any obligation whatsoever; and the fact that the Government may have formulated, furnished, or in any way supplied the said drawings, specifications, or other data, is not to be regarded by implication or otherwise as in any manner licensing the holder or any other person or corporation, or conveying any rights or permission to manufacture, use, or sell any patented invention that may in any way be related thereto.

Copies of this report should not be returned to the Research and Technology Division unless return is required by security considerations, contractual obligations, or notice on a specific document.

9 **FINAL REPORT**, Mar - Nov 66,

6 **DEVELOPMENT OF HIGH PERFORMANCE POROUS TUNGSTEN IONIZERS.**

11 **NOVEMBER 1966** (12) (66p.)

14 05823-6005-R000

18 AFML

19 TR-67-21

Metallurgical Processing Branch
Manufacturing Technology Division
Air Force Material Laboratory
Research and Technology Division
Air Force Systems Command
United States Air Force
Wright-Patterson Air Force Base, Ohio

This document is subject to special export controls and each transmittal to foreign governments or foreign nationals may be made only with prior approval of the Manufacturing Technology Division.

16 MMP-9-188

15
(Prepared under Contract AF 33(615)-3817 by

TRW (354 595)
SYSTEMS GROUP

10 M. E. Kirkpatrick and R. A. Mendelson (Authors)

msk

FOREWORD

This final technical report covers all of the work performed under Contract AF33(615)-3817 from March 1966 through November 1966. This manuscript was released by the authors on 15 December 1966 for publication as an RTD Technical Report.

This contract with TRW Systems, Redondo Beach, California, was initiated under Manufacturing Methods Project 9-188, "Development of Porous Tungsten Ion Emitter Processing." This program was accomplished under technical direction of Mr. G. A. Gegel of the Metallurgical Processing Branch, Manufacturing Technology Division, Air Force Materials Laboratory, Wright-Patterson Air Force Base, Ohio.

Mr. M. E. Kirkpatrick, Manager of the Crystal and Surface Physics Department, Systems Laboratories, TRW Systems, was in charge of the program. Others who were active in the research and preparation of this report are R. A. Mendelson, K. Staudhammer, and J. L. Reger.

This project has been accomplished as a part of the Air Force Manufacturing Methods program, the primary object of which is to develop on a timely basis manufacturing processes, techniques, and equipment for use in economical production of USAF materials and components. The program encompasses the following technical areas:

- Metallurgy - Rolling, Forging, Extruding, Casting, Fiber, Powder.
- Chemical - Propellant, Coating, Ceramic, Graphite, Nonmetallics.
- Fabrication - Forming, Material Removal, Joining, Components.
- Electronics - Solid State, Materials and Special Techniques, Thermionics.

Suggestions concerning additional Manufacturing Methods development required on this or other subjects will be appreciated.

This technical report has been reviewed and is approved.

Melvin E. Fields

MELVIN E. FIELDS
Colonel, USAF
Chief, Manufacturing Technology Division
AF Materials Laboratory

ABSTRACT

A development program directed toward the further development of techniques involved in the preparation and testing of porous tungsten ionizer materials is described. A current state-of-the-art survey is included to establish the status of porous ionizer material technology.

Experimental results relating to particle size distribution and to the pore parameters of the resulting compacts are presented. Parameters such as sintering time and temperature, density, porosity, permeability, thermal stability, and ionizer performance were studied. The results of all the experimental investigations along with a description of the experimental approach are presented in this report.

TABLE OF CONTENTS

	<u>Page</u>
I. INTRODUCTION	1
II. REVIEW OF IONIZER DEVELOPMENT PROGRAMS	2
III. EXPERIMENTAL INVESTIGATIONS.	5
A. Powder Procurement.	5
B. Powder Evaluation	5
C. Compaction and Sintering.	14
D. Compact Analysis and Evaluation	18
IV. DISCUSSION AND REVIEW.	45
V. SUMMARY.	65

LIST OF ILLUSTRATIONS

<u>Figure</u>		<u>Page</u>
1	Photomicrograph of the Federal Mogul Powder Lot FM-1. X1000. .	7
2	Photomicrograph of the Federal Mogul Powder Lot FM-2. X1000. .	7
3	Photomicrograph of Union Carbide Powder Lot UC-3 Showing the -0% Powder Fraction. X1000.	8
4	Photomicrograph of Union Carbide Powder Lot UC-3 Showing the -1% Powder Fraction. X1000.	8
5	Photomicrograph of Union Carbide Powder Lot UC-3 Showing the +1% Powder Fraction. X1000.	9
6	Photomicrograph of Union Carbide Powder Lot UC-3 Showing the +8% Powder Fraction. X1000.	9
7	Photomicrograph of Union Carbide Powder Lot UC-3 Showing the +10% Powder Fraction. X1000	10
8	Photomicrograph of Union Carbide Powder Lot UC-3 Showing the +15% Powder Fraction. X1000	10
9	Photomicrograph of Union Carbide Powder Lot UC-3 Showing the +20% Powder Fraction. X1000	11
10	Photomicrograph of Union Carbide Powder Lot UC-3 Showing the +25% Powder Fraction. X1000	11
11	Photomicrograph of Union Carbide Powder Lot UC-3 Showing the +30% Powder Fraction. X1000	12
12	Photomicrograph of Union Carbide Powder Lot UC-3 Showing the +37% Powder Fraction. X1000	12
13	Photomicrograph of Porous Ionizer Compact FM 1-3 at 1000X. % of Theoretical Density = 71.4.	19
14	Photomicrograph of Porous Ionizer Compact FM 1-4 at 1000X. % of Theoretical Density = 76.4.	19
15	Photomicrograph of Porous Ionizer Compact FM 2-1 at 1000X. % of Theoretical Density = 75.3.	20
16	Photomicrograph of Porous Ionizer Compact FM 2-2 at 1000X. % of Theoretical Density = 71.0.	20

ILLUSTRATIONS (Continued)

<u>Figure</u>		<u>Page</u>
17	Photomicrograph of Porous Ionizer Compact UC 3-5 at 1000X. % of Theoretical Density = 75.5	21
18	Photomicrograph of Porous Ionizer Compact UC 3-8 at 1000X. % of Theroetical Density = 72.1	21
19	Relationship Between Porosity and Specific Permeability for Powder Lot UC-3	26
20	An Overall View of the Ion Emitter Module Used During This Program.	28
21	Surface of Ionizer After Eloxing	29
22	Surface of Ionizer After Eloxing and Electropolishing	29
23	The Relationship Between Cesium Neutral Fraction as Percent Neutrals Versus Emitter Temperature in Degrees K for the Ionizer Compact FM 1-3.	32
24	The Relationship Between Cesium Neutral Fraction as Percent Neutrals Versus Emitter Temperature in Degrees K for the Ionizer Compact FM 1-4.	33
25	The Relationship Between Cesium Neutral Fraction as Percent Neutrals Versus Emitter Temperature in Degrees K for the Ionizer Compact FM 2-1.	34
26	The Relationship Between Cesium Neutral Fraction as Percent Neutrals Versus Emitter Temperature in Degrees K for the Ionizer Compact FM 2-2.	35
27	The Relationship Between Cesium Neutral Fraction as Percent Neutrals Versus Emitter Temperature in Degrees K for the Ionizer Compact UC 3-8.	36
28	The Relationship Between Cesium Neutral Fraction as Percent Neutrals Versus Emitter Temperature in Degrees K for the Ionizer Compact UC 3-5.	37
29	Relationship Between Ionizer Lifetimes and Temperature for Powder Lots FM-1 and UC-3	39
30	Densification Curve for a 3.6 Micron Powder Showing a Rapid Increase in Density During the Early Stages of Sintering. . .	40

ILLUSTRATIONS (Continued)

<u>Figure</u>		<u>Page</u>
31	Densification Curve for Powder Lot FM-1 at 1700° K Showing a Rapid Increase in Density During the Early Resintering and a Lower Rate of Densification in the Later Resintering.	41
32	Cut-Away View of the Powder Compacting Die Showing the Double Insert Configuration.	49
33	"Green" Density as a Function of Compacting Pressure for Various Types of Compaction Methods.	50
34	Sintering Rates at Various Temperatures for Powder Lot 3 . . .	53
35	Arrhenius Plot of Sintering Rate for Powder Lots 3, 7, and 9.	54
36	Relationship Between the Sintering Rate and Reciprocal Surface Area for the Temperatures Shown.	55
37	Typical Photomicrograph of a Porous Structure From Powder Lot 3. X1000.	56
38	The Observed Surface Pore Densities as a Function of Particle Size Shown in Relation to (a) the Expected Values if Ideal Packing of Uniform Spheres Were Realized, and (b) the Typical Values for Non-Spherical Powder.	59
39	Relationship Between Porosity and Specific Permeability for Powder Lot 3	61
40	Photograph of an Emitter Module Used for Cesium Ionization Testing.	62
41	Observed Relationship Between Cesium Neutral Fraction and Ion Current Density for Spherical Tungsten Powder Ionizers Investigated	63

LIST OF TABLES

<u>Table</u>		<u>Page</u>
I	Designation and Supplier of Spherical Tungsten Powder . . .	6
II	Weight and Number Percentages of Powder Lots FM-1, FM-2, and UC-3.	13
III	Summary of the Statistical Analysis of Powder Lots FM-1, FM-2, and UC-3.	15
IV	Summary of Union Carbide's Classification of Powder	16
V	Summary of Compacts Fabricated Using a Compacting Pressure of 35,000 psi.	17
VI	Values of Pore Parameters for the Low Density Ionizer Test Buttons.	22
VII	Results of Permeability Analysis Conducted on the Ionizer Test Module	24
VIII	Permeability as a Function of Sintering Time at 2000° C For Compact UC 3-7.	25
IX	Relative Density Change for Vacuum Stability Samples After 200 Hours at 50-Hour Intervals.	43
X	Typical Impurity Levels of Tungsten Powders as Determined by Spectrographic Analyses	46
XI	Powder Parameters	47
XII	Sintered Densities for Three Powder Lots Investigated . . .	52
XIII	Porosity and Permeability Parameters for Several Types of Porous Materials Investigated.	58

I. INTRODUCTION

The primary objective of the current program was to further develop the techniques involved in the production of porous tungsten ionizer materials and to more fully characterize the emitter material produced in the actual operational environment of an ion engine. This program was an extension of the work performed by this laboratory under Air Force contract AF 33(657)-11726.⁽¹⁾ The current laboratory investigations involve the study of three separate lots of spherical tungsten powders. The first two of these powder types were produced by independent methods and have an average particle size between three and four microns with a standard deviation of approximately one micron. The third powder type has an average particle diameter between three and four microns and a standard deviation of 0.8 microns. All porous materials were processed in a fashion similar to that used in the preceding program. Following the accepted test procedures, all ionizer materials were characterized with respect to pore size, surface pore density, interpore spacing, pore distribution and uniformity, and permeability. The primary test objectives of this laboratory investigation include the determination of long-term dimensional stability over the range of ionizer temperatures anticipated in an engine environment. Dimensional stability tests were run in a vacuum environment at temperatures at 1300, 1400, 1500, and 1700° K for extended time periods to determine the variation of both permeability and porosity as a function of time. In addition, an investigation of the dimensional stability and resulting permeability variations for each of the porous material types was carried out under actual engine environmental conditions using a cesium flow rate equivalent to operational conditions. These investigations were carried out at temperatures in the range of 1400-1500° K for extended time periods to determine the variation in cesium permeability as a function of time. In addition, ionizer buttons having an emitter area of 2.5 cm² have been evaluated over a range of ion current densities up to 40 ma/cm².

II. REVIEW OF IONIZER DEVELOPMENT PROGRAMS

During the past few years, several laboratories have been actively involved with programs to develop high performance porous ionizer materials. In general, all programs have been based on powder metallurgy techniques for the production of porous bodies suitable for ionizer use. In all cases, the trend has been toward the use of closely-sized spherical tungsten powders as a starting point for the production of these materials. The use of spherical powders has produced significant gains in the performance of ionizer materials, and it is generally considered that the benefits have resulted from greater uniformity in the parameters related to the pore structure and porosity of these materials.

A series of laboratory investigations carried out by Hughes Research Laboratories^(2,3) have resulted in the development, production, and evaluation of both pure tungsten and tungsten-alloy porous ionizer materials. Tungsten ionizers exhibiting surface pore densities approaching 10 million pores/cm² have been studied, and the variation in ionizer performance with surface pore densities and starting particle size have been determined. Powder compacts were prepared by "warm" pressing billets of flat plate geometry using a powder die of conventional design. Compacts were vacuum sintered to a density equal to 80 percent of theoretical. Studies have involved pore parameters, permeability, dimensional stability, and ionizer performance. In addition, selected tungsten base alloy ionizers and surface coatings have been investigated and evaluated.

Investigations performed by Electro-Optical Systems^(4,5) have been aimed at the determination of the effects of alloy additions on the stability of porous ionizer materials. These studies have involved both mechanical mixtures and prealloyed spherical powders and have produced data relating to additions of tantalum, rhenium, and iridium to tungsten-base powder compacts. Porous materials again exhibiting surface pore densities in the range of 10 million pores/cm² have been produced and evaluated. The data for spherical powder compacts reveal a general correlation between ionizer performance and surface pore densities.

In addition, a separate laboratory effort is currently in progress by R. Neal and others⁽⁶⁾ to investigate and develop ionizer processing techniques. These studies involve both pure tungsten microspheres as well as prealloyed tungsten-rhenium microspheres.

It is clear from the published data of these laboratory investigations that a significant benefit is derived with regard to ionizer elevated temperature dimensional stability through the addition of alloying elements such as tantalum, rhenium, and iridium. In the case of tantalum additions, it would appear that the greatest stability is derived from a 10 atomic addition. Systematic data relating to rhenium additions are not yet available, but it has been demonstrated that some enhancement of stability does result from the addition of small amounts of rhenium.

In general, all laboratory programs involved in the development of porous ionizer materials have used sintering times and temperatures sufficient to bring the porous material to 80 percent of theoretical density; thus, all starting porosities have been in the range of 20 percent. Recent data⁽⁵⁾ are now available for materials with substantially greater initial porosity. These data reveal ionizer performance which equals that of the highest surface pore density materials made to date. However, the surface pore densities observed for the high porosity materials is substantially less than the 10 million pores/cm² prepared from spherical tungsten powders. Based on data such as these, as well as the observed ionizer performance as a function of powder size during the preceding experimental effort in this laboratory, it would appear that systematic data relating to ionizer performance as a function of porosity are almost totally absent from the several published laboratory investigations.

In summary, it is apparent that substantial gains have been realized by the several laboratories working in the area of ionizer materials development through the use of closely-classified spherical powders. From the available data, it is believed that this gain has been primarily a result of

the enhanced uniformity of the porosity and permeability of these materials. The data which attempt to correlate ionizer performance with pore diameter and surface pore density are not consistent; and the more recent data, in fact, suggest no direct correlation of performance with surface pore density. It has been demonstrated by several investigators that the dimensional stability of porous compacts can be enhanced through the addition of alloying elements such as tantalum, rhenium, and iridium without significantly effecting ionizer performance.

III. EXPERIMENTAL INVESTIGATIONS

A. Powder Procurement

Based on a survey of suppliers of spherical tungsten powders, procurement was initiated with the Crystal Products Division of Union Carbide and with the Federal Mogul Corporation for the powders listed in Table I. Two separate lots of spheroidized powder were ordered from Federal Mogul. These powder lots were specified to have an average particle size of 3.5 microns with standard deviations of 1.0 and 0.5 microns, respectively. The Union Carbide powder was obtained as an unclassified powder lot with subsequent classification accomplished by Union Carbide at the Oak Ridge facility. In every case, the powders were classified using a Vortec air classifier. Figures 1 and 2 show typical photomicrographs of the powders as received from Federal Mogul. A preliminary analysis of the Federal Mogul powder indicated that the quantity of agglomerates and submicron particles exceeded the specified value. As a result, powder lot FM-1 was returned for further processing and reclassification to yield a powder with an acceptable quantity of fine particles. Figures 3 through 12 are photomicrographs representing each of the fractions of the classifier output for the powder from Union Carbide.

B. Powder Evaluation

Evaluation of all of the powder was accomplished by use of complete visual examination. This examination consisted of a particle count taken from 1000 diameter photomicrographs using a template specially designed for the purpose of determining the particle diameter. From each of the powder lots, at least 600 individual particles were counted. The raw data that was obtained was then changed into useful percentage numbers using standard statistical methods. The information gained from these data are the percent by weight and by number. Also, the average particle size both by weight and by number was calculated. In addition, the standard deviation of each of the powder lots was then calculated. Table II is a summary of the powder analysis showing the comparison between weight and number percentages.

Table I

Designation and Supplier of Spherical Tungsten Powder

<u>TRW Designation</u>	<u>Supplier</u>	<u>Ordered Sizes</u>
FM-1	Federal Mogul	3.0 - 3.5 μ \pm 1 μ
FM-2	Federal Mogul	3.0 - 3.5 μ \pm 1/2 μ
UC-3	Union Carbide	75 w/o < 10 μ 32 w/o between 2 and 5 μ

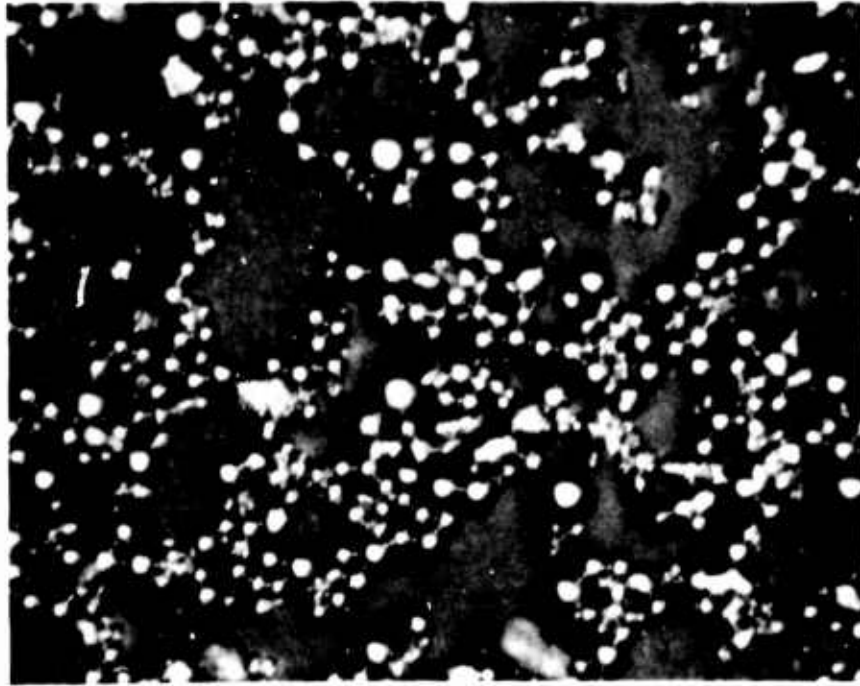


Figure 1. Photomicrograph of the Federal Mogul Powder Lot FM-1. X1000

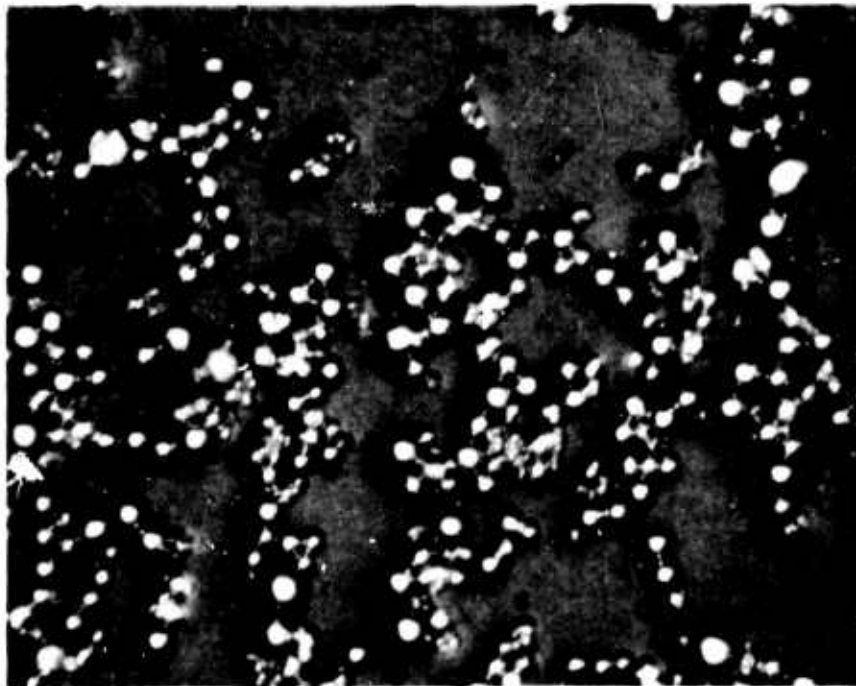


Figure 2. Photomicrograph of the Federal Mogul Powder Lot FM-2. X1000

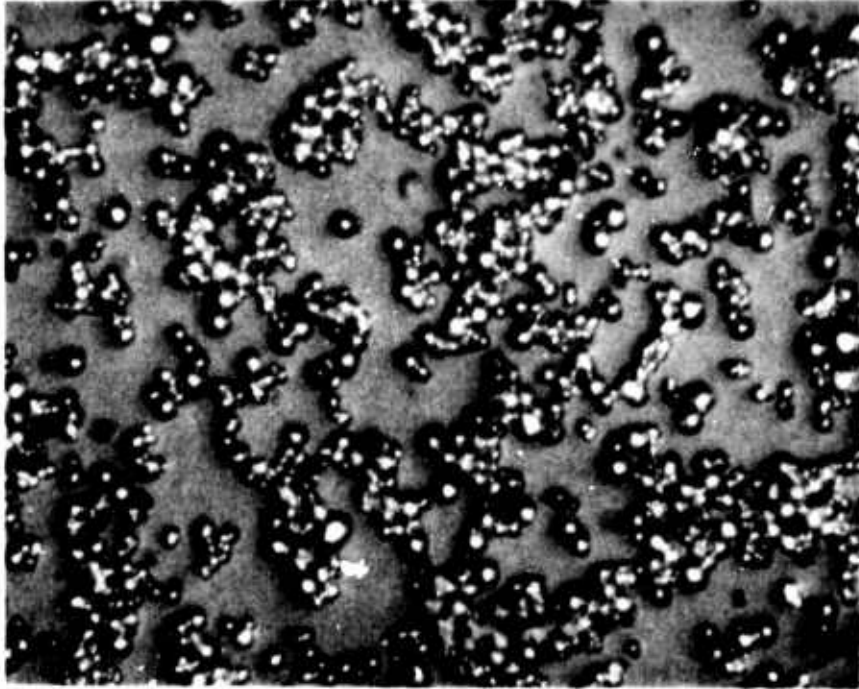


Figure 3. Photomicrograph of Union Carbide Powder Lot UC-3 Showing the -0% Powder Fraction. X1000

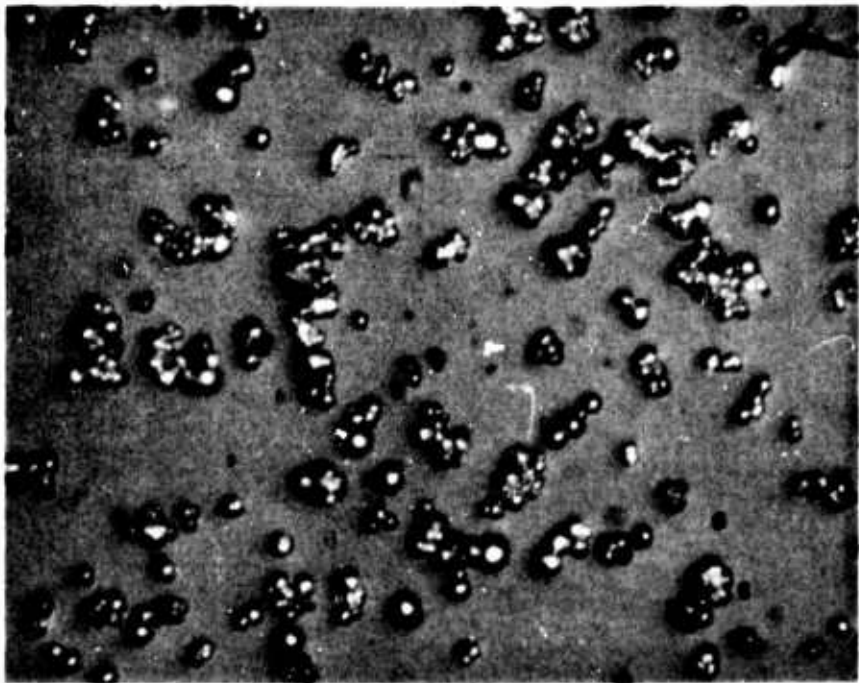


Figure 4. Photomicrograph of Union Carbide Powder Lot UC-3 Showing the -1% Powder Fraction. X1000

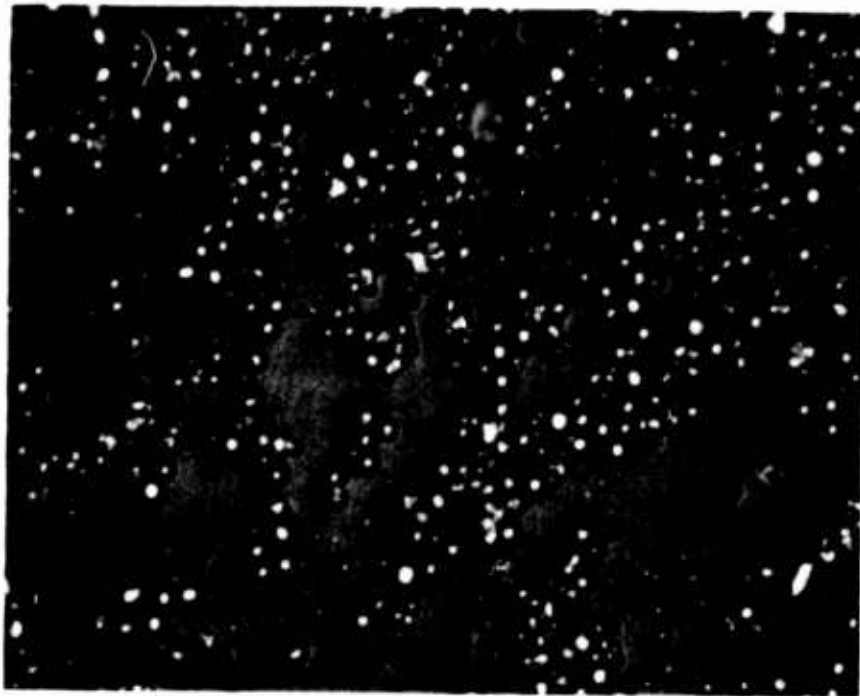


Figure 5. Photomicrograph of Union Carbide Powder Lot UC-3 Showing the +1% Powder Fraction. X1000

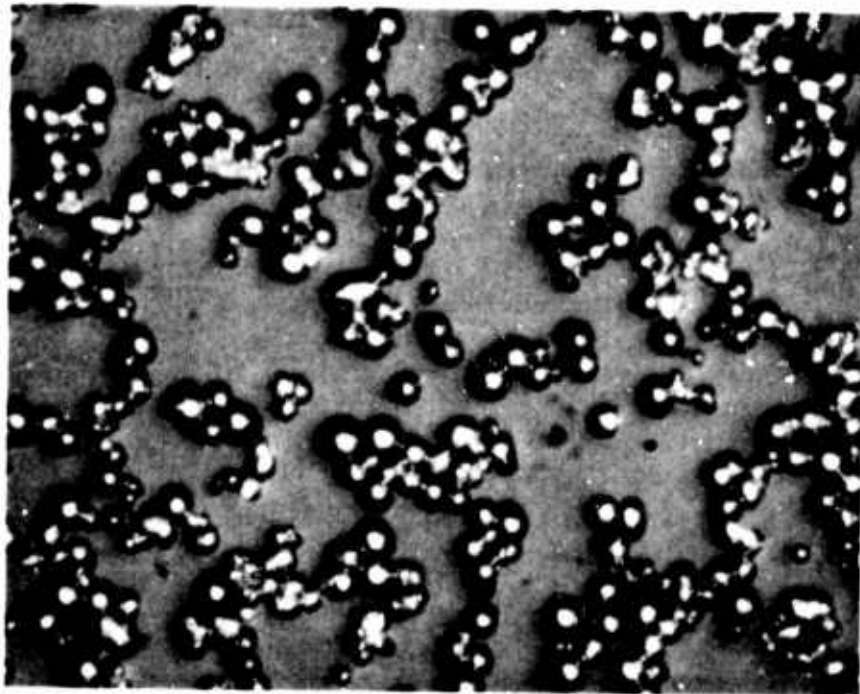


Figure 6. Photomicrograph of Union Carbide Powder Lot UC-3 Showing the +8% Powder Fraction. X1000

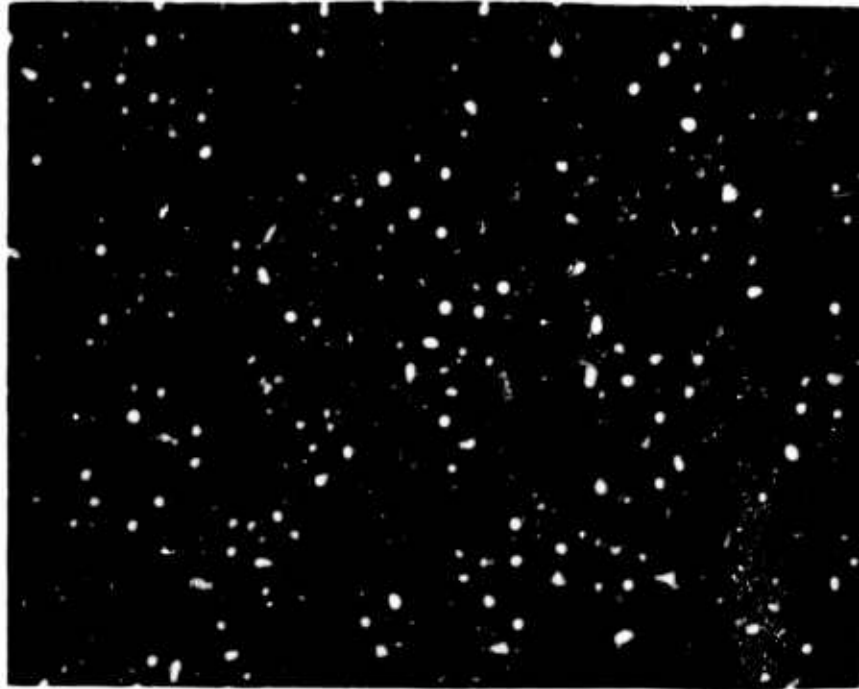


Figure 7. Photomicrograph of Union Carbide Powder Lot UC-3 Showing the +10% Powder Fraction. X1000

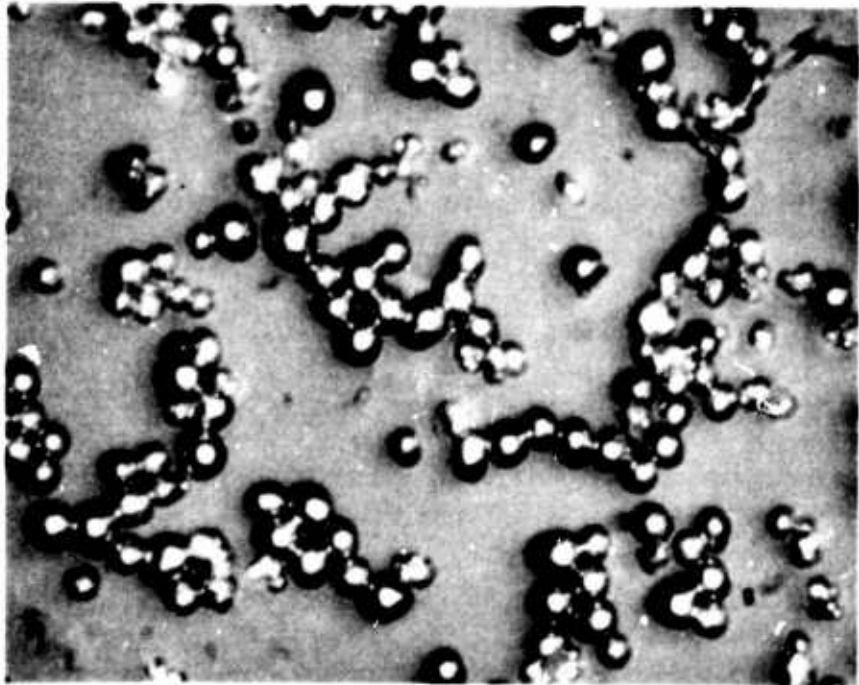


Figure 8. Photomicrograph of Union Carbide Powder Lot UC-3 Showing the +15% Powder Fraction. X1000

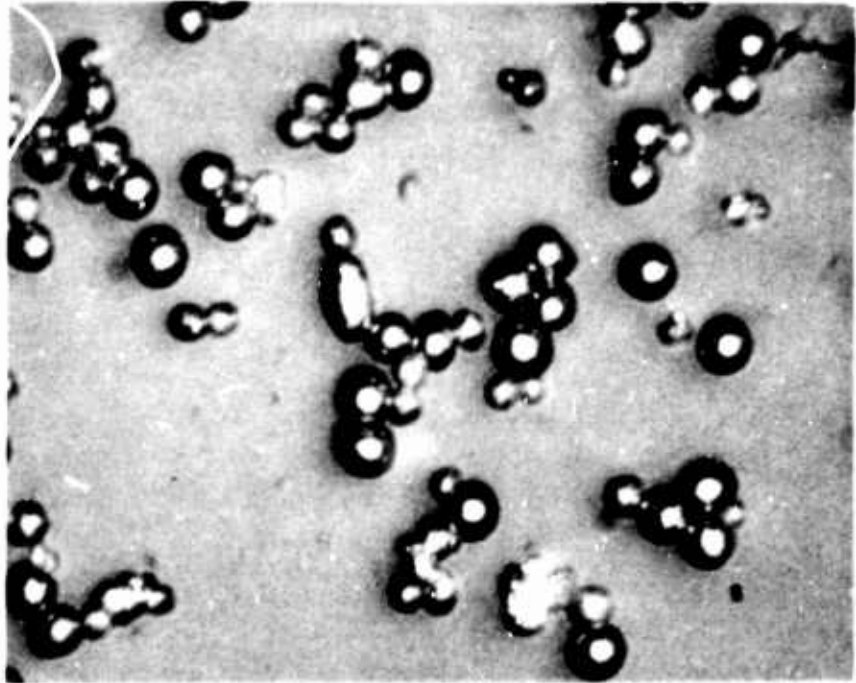


Figure 9. Photomicrograph of Union Carbide Powder Lot UC-3 Showing the +20% Powder Fraction. X1000



Figure 10. Photomicrograph of Union Carbide Powder Lot UC-3 Showing the +25% Powder Fraction. X1000

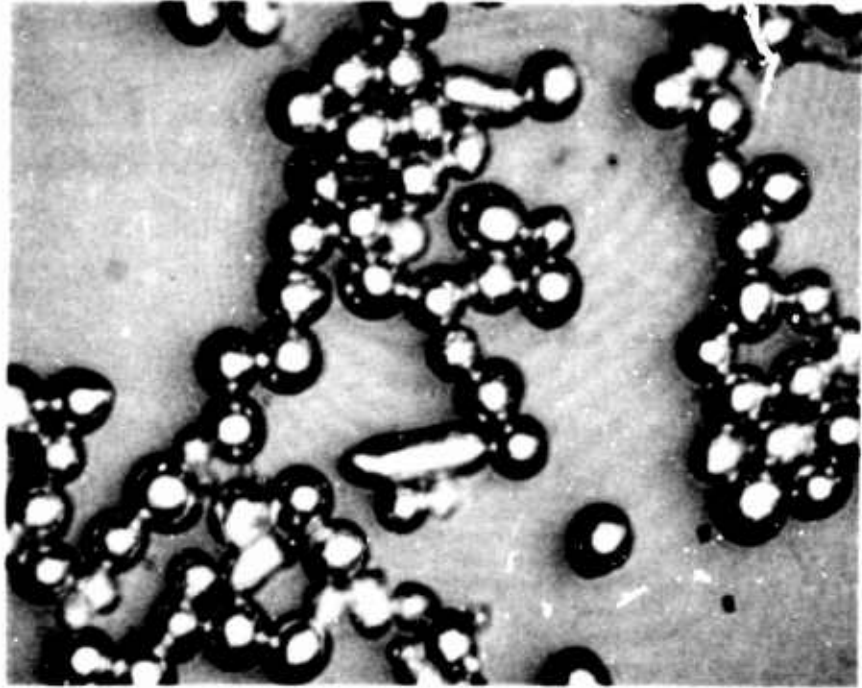


Figure 11. Photomicrograph of Union Carbide Powder Lot UC-3 Showing the +30% Powder Fraction. X1000

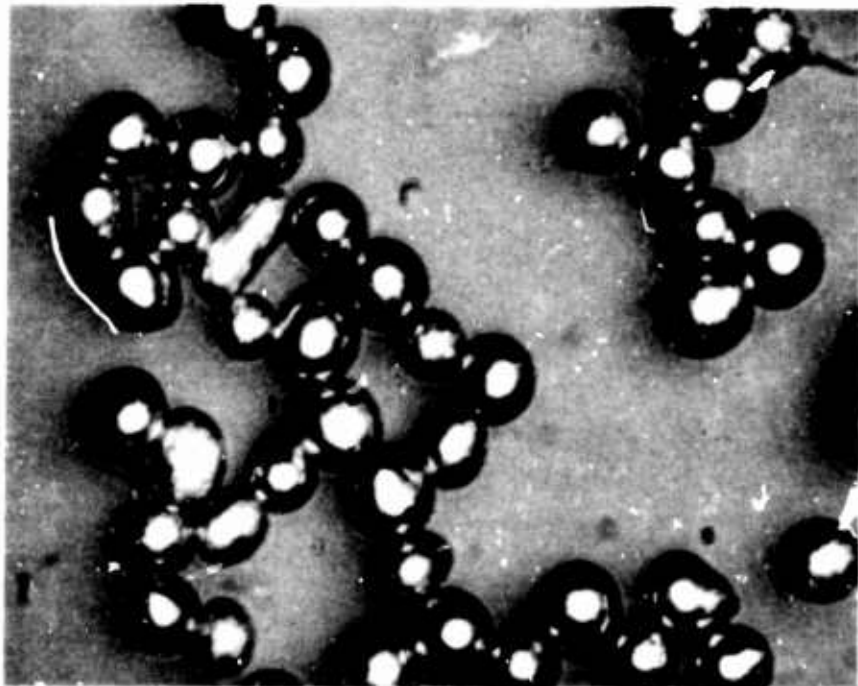


Figure 12. Photomicrograph of Union Carbide Powder Lot UC-3 Showing the +37% Powder Fraction. X1000

Table II

Weight and Number Percentages
of Powder Lots FM-1, FM-2, and UC-3

Particle Size	FM-1		FM-2		UC-3	
	Number %	Weight %	Number %	Weight %	Number %	Weight %
1	9.4	.4	10.8	.5	4.4	.1
1.5	15.0	2.4	16.8	2.6	10.5	.8
2	17.0	6.5	17.7	6.5	12.3	2.2
2.5	20.7	15.5	18.5	13.3	12.6	4.5
3	18.6	24.0	15.0	18.5	13.8	8.4
3.5	13.4	27.5	11.0	21.5	13.3	12.9
4	3.9	12.0	5.8	17.0	13.9	20.3
4.5	1.0	4.4	3.4	14.1	9.9	20.4
5	.6	3.6	.3	1.8	6.0	17.0
5.5	.2	1.6	.3	2.5	2.5	9.2
6	.2	2.1	.2	1.6	.8	4.0

Table III is the statistical results of the analysis in terms of average particle size and standard deviation of each of the powder lots.

Additional examination of the Union Carbide powder in the form of a micromerograph were performed by Union Carbide. These data are presented as Table IV.

C. Compaction and Sintering

As a result of the technical literature survey carried out during the initial portion of this program, it was decided to employ a compaction process identical to that used in the preceding Air Force sponsored program. This compaction method employs the use of a double elastomeric insert. The internal insert (the material adjacent to the tungsten powder) is a soft (30 shore hardness) elastic material which under pressure acts as a semi-liquid to produce near-isostatic conditions in the powder cavity. The outer material which completely encloses the inner material is a polyurethane material which is relatively hard (80 shore) and abrasion resistant. This outer material prevents extrusion of the soft inner material between the punch and die walls. A compaction pressure of 35,000 psi was selected to provide "green" compacts that had minimum density with enough strength to be handled easily.

Sintering operations for the tungsten compacts were performed in a vacuum environment using a resistively-heated tantalum-10 w/o tungsten furnace element. During the sintering operations, the tungsten billets were enclosed by tungsten plates in order to reduce or eliminate any line of sight impurities from the furnace walls or the heating elements. The sintering times and temperatures used were sufficient to produce sintered compacts exhibiting densities near 75 percent of theoretical. A total of 25 porous tungsten ionizer billets were produced during this program. Table V provides a summary of the compacts produced with the associated sintering history.

Table III

Summary of the Statistical Analysis
Of Powder Lots FM-1, FM-2, and UC-3

Average Particle Size	FM-1	FM-2	FM-3
By Weight	3.3	3.4	4.2
By Number	2.5	2.4	3.1
Standard Deviation	.89 μ	.81 μ	1.18 μ

Table IV

Summary of Union Carbide's Classification of Powder

<u>Cut Designation (Vortec Settings)</u>	<u>Micromerograph* Particle Size, Microns</u>	<u>Yield g</u>	<u>Loss g</u>
-0%	2.7	150	36
-1	2.7	211	67
+1	2.7	2,157	--
+8	3.7	564	15
+10	3.8	565	16
+15	4.6	2,584	27
+20	5.8	876	17
+25	6.6	635	25
+30	7.8	1,153	46
+37	13.0	1,005	36

*Microscopic examination by Union Carbide suggests that the average particle size by count was 1/2 to 1 micron higher than that indicated by micromerograph.

Table V

Summary of Compacts Fabricated Using
A Compacting Pressure of 35,000 psi

<u>Powder Lot</u>	<u>Compact</u>	<u>Sintering Temperature ° C</u>	<u>Sintering Time Hours</u>	<u>% Theoretical Density</u>
FM-1	1	1900	1 1/2	76.3
	2	1900	1 1/2	77.0
	3	1900	1 1/2	75.8
	4	1900	2	79.7
	5	1900	2	75.4
	6	1900	1 3/4	76.8
	7	1900	1 3/4	76.8
FM-2	1	1900	6 1/2	80.6
	2	1900	6 1/2	76.3
	3	2000	1 3/4	75.9
	4	2000	1 3/4	76.3
	5	2000	1 3/4	76.8
UC-3	1	1900	4	75.6
	2	1900	3 1/4	76.3
	3	1900	4	76.1
	4	2000	1 3/4	76.1
	5	2000	2 1/2	80.0
	6	2000	1 3/4	76.3
	7	2000	1 1/2	75.2
	8	2000	1 3/4	76.2
	9	2000	2	76.4
	10	2000	2	75.7
	11	2000	3 1/4	77.0
	12	2000	3 3/4	77.9
	13	2000	2 1/4	76.1

D. Compact Analysis and Evaluation

1. Metallography

Metallographic investigations were carried out on porous compacts from each of the powder lots. The purpose of these investigations was to determine such pore parameters as pore shape, size, uniformity, and surface pore density. Photomicrographs are presented as Figures 13 through 18 representing typical observed microstructures for all of the powder lots. From photomicrographs such as those shown, pore counts were performed to determine the surface pore density.

The data pertaining to surface pores were obtained by the direct pore count method. This method consists of a physical count of the pores as observed on a 1000 diameters photomicrograph using a circular template prepared for these measurements. Since actual pore shapes and configurations deviate from the idealized case of circular pores, the surface pore density data presented in this report were obtained using the approximation that elongated pores may be counted as multiple pores equal to the number of average pore diameters represented by the elongation. Table VI summarizes the pore parameters of the porous tungsten evaluated during this program.

2. Permeability

Permeability measurements were taken on the ionizer test modules and on other billets of the porous tungsten. The measurements were based on gas flow data as a function of differential pressure. The relation for specific permeability as defined by Darcy's Law⁽⁷⁾ is

$$k = \frac{q\mu}{A(\Delta P/L)}$$

where: q = fluid flow rate
μ = viscosity of fluid
A = cross-sectional area
ΔP = pressure differential
L = thickness

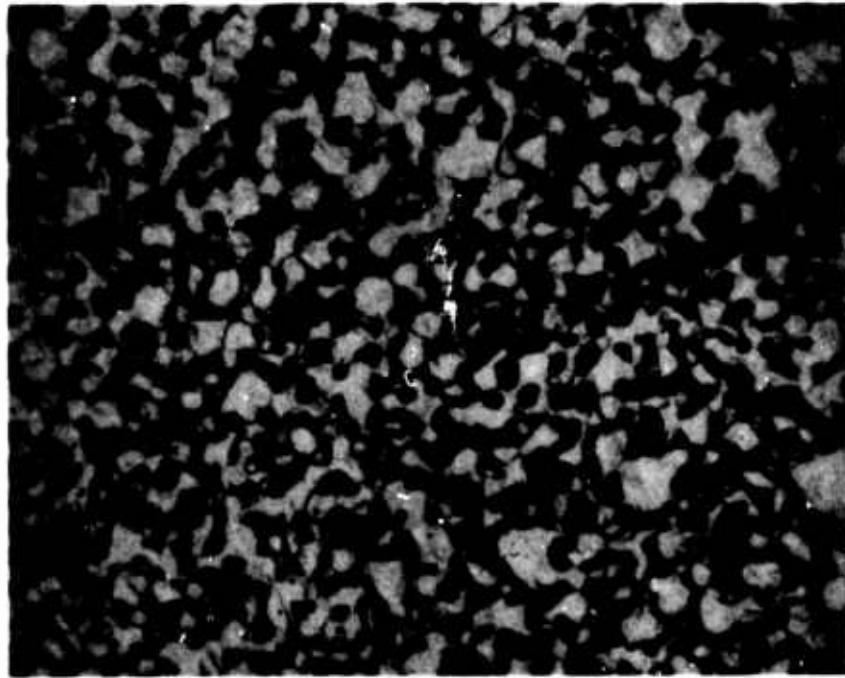


Figure 13. Photomicrograph of Porous Ionizer Compact FM 1-3 at 1000X. % of Theoretical Density = 71.4.

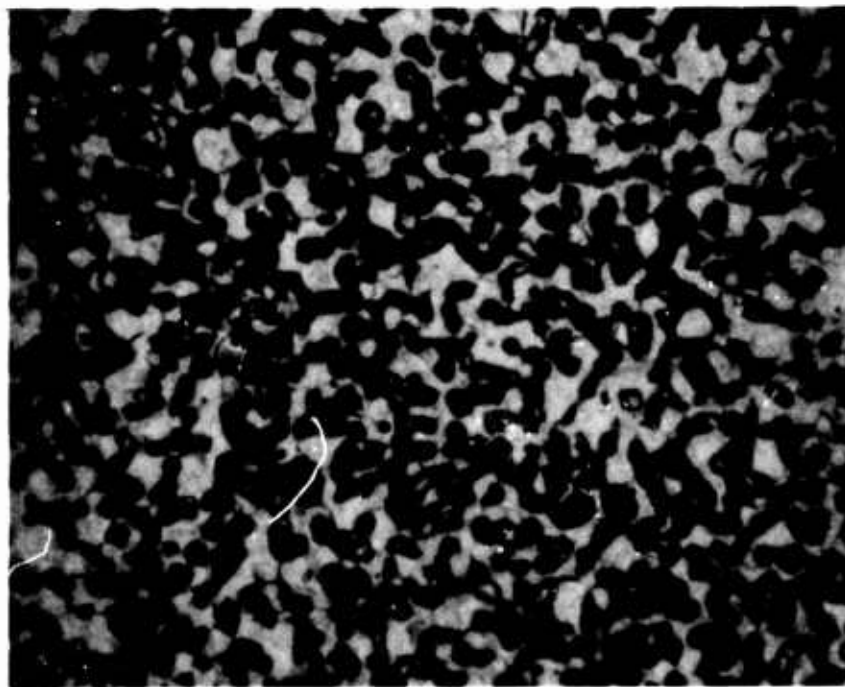


Figure 14. Photomicrograph of Porous Ionizer Compact FM 1-4 at 1000X. % of Theoretical Density = 76.4.

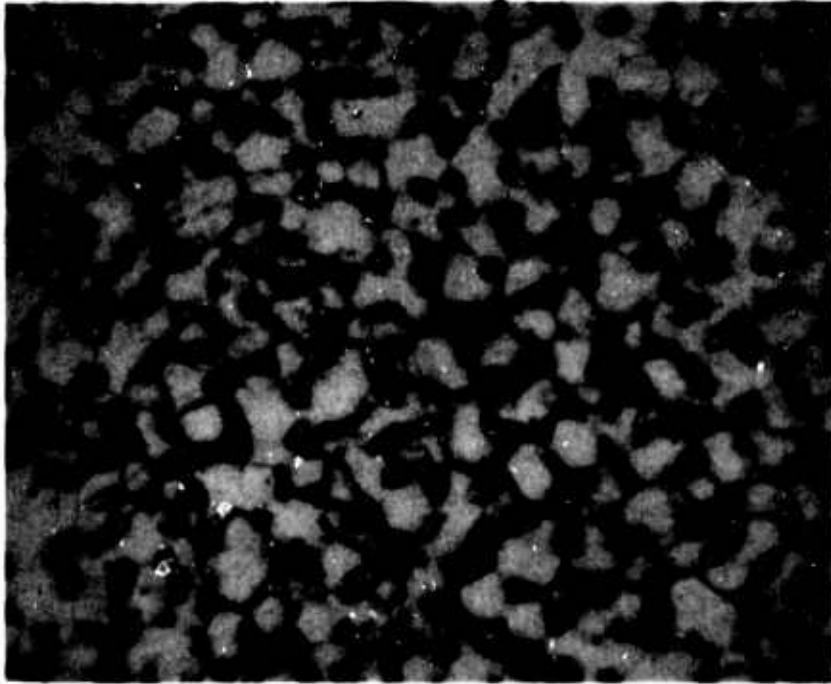


Figure 15. Photomicrograph of Porous Ionizer Compact FM 2-1 at 1000X. % of Theoretical Density = 75.3.

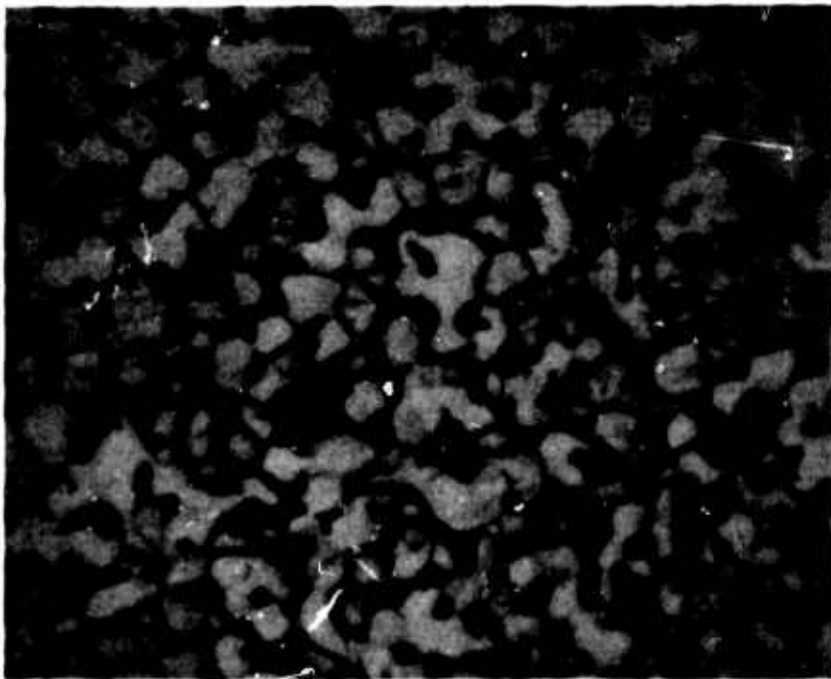


Figure 16. Photomicrograph of Porous Ionizer Compact FM 2-2 at 1000X. % of Theoretical Density = 71.0.

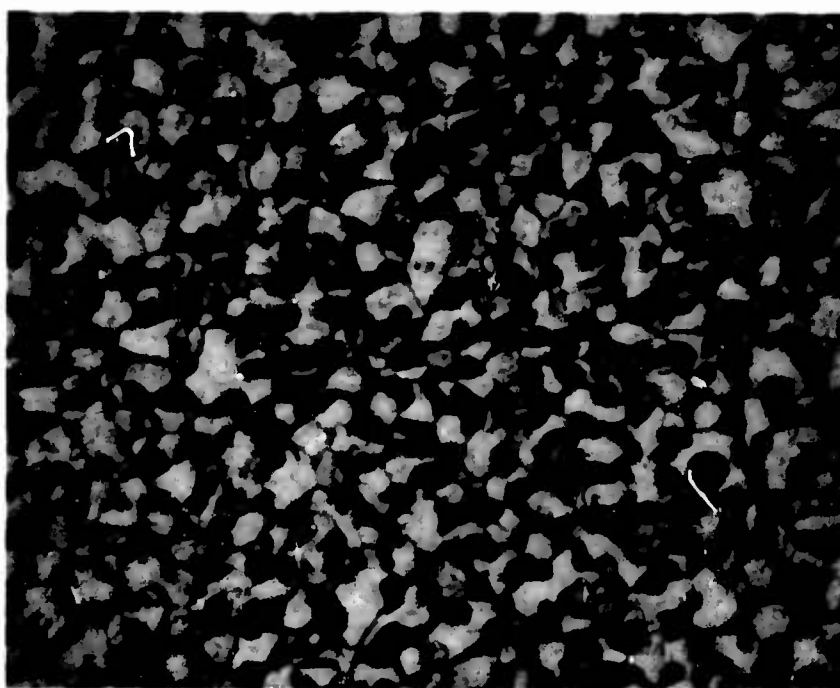


Figure 17. Photomicrograph of Porous Ionizer Compact UC 3-5 at 1000X. % of Theoretical Density = 75.5.

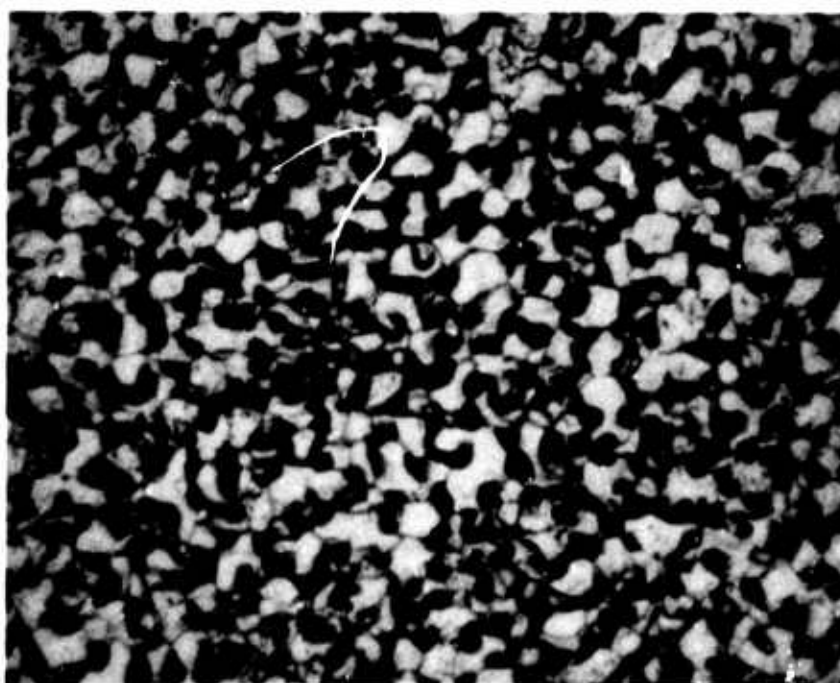


Figure 18. Photomicrograph of Porous Ionizer Compact UC 3-8 at 1000X. % of Theoretical Density = 72.1.

Table VI

Values of Pore Parameters for the Low
Density Ionizer Test Buttons

	FM-1	FM-2	UC-3
Pore Diameter	1.91 μ	2.07 μ	1.82 μ
Surface Pore Density (pores/cm ²)	8.0 x 10 ⁶	5.75 x 10 ⁶	8.4 x 10 ⁶

It should be noted that the units of specific permeability are length squared. Therefore, the specific permeability is related to the effective cross-sectional area of the porous body and is independent of the nature of the flowing fluid. The results of these permeability examinations are presented as Table VII.

In addition to the permeability testing carried out on the ionizer buttons, one billet was tested to determine the decrease in permeability as the density increased. These data are presented in Table VIII and graphically in Figure 19. The observed relationships show that a change of 2 1/2 orders of magnitude in specific permeability is encountered in a change of porosity (or density) of less than 20 percent. This type of evaluation is useful in that it provides information about the permeability of a compact at any given density within similar powder lots. Knowing the permeability density relationship, extrapolation of the lifetimes can be made with greater certainty. This particular aspect of these investigations will be covered in the section on thermal stability.

3. Ionizer Testing

a. Ionizer Module Fabrication

All ionizer tests were performed on 0.700 inch diameter specimens which were machined from the full size compacts produced. The 0.700 inch diameter buttons produced an effective emitting area of 2.5 cm². The test specimens were fabricated from porous tungsten compacts representing the three powder lots prepared at two different densities which produce six test samples.

The test modules used in this program consisted of a rectangular solid tungsten plenum having the dimension of 1" x 2" with the porous tungsten buttons located centrally within each end half of the tungsten slab. The buttons were recessed and positioned directly over a cesium plenum chamber which was connected to the cesium supply by separate 0.125 inch

Table VII
Results of Permeability Analysis Conducted
On the Ionizer Test Module

<u>Powder Lots</u>	<u>Density</u>	<u>Specific Permeability</u>
FM-1	71.4	$9.8 \times 10^{-11} \text{ cm}^2$
	76.4	$4.5 \times 10^{-11} \text{ cm}^2$
FM-2	71.0	$2.0 \times 10^{-10} \text{ cm}^2$
	75.3	$1.3 \times 10^{-10} \text{ cm}^2$
UC-3	75.5	$6.3 \times 10^{-11} \text{ cm}^2$
	72.1	$1.2 \times 10^{-10} \text{ cm}^2$

Table VIII

Permeability as a Function of Sintering Time

At 2000° C for Compact UC 3-7

<u>Sintering Time</u>	<u>Density</u>	<u>Permeability</u>	<u>% of K_0</u>
1.5 hrs.	72.2	$1.20 \times 10^{-10} \text{ cm}^2$	100
2.0	74.3	7.8×10^{-11}	65.0
2.5	75.4	6.6×10^{-11}	55.0
3.0	76.6	5.6×10^{-11}	46.7
3.5	77.6	4.0×10^{-11}	33.3
4.5	79.3	2.9×10^{-11}	24.2
5.5	80.8	1.7×10^{-11}	14.2
7.5	82.6	1.0×10^{-11}	8.33
9.5	84.0	7.27×10^{-12}	6.1
11.5	85.1	4.27×10^{-12}	3.6
13.5	86.2	2.1×10^{-12}	1.7
15.5	87.2	1.12×10^{-12}	.93
17.5	88.0	7.5×10^{-13}	.62
19.5	88.6	4.3×10^{-13}	.36
21.5	89.2	4.25×10^{-13}	.35
23.5	89.8	4.2×10^{-13}	.35

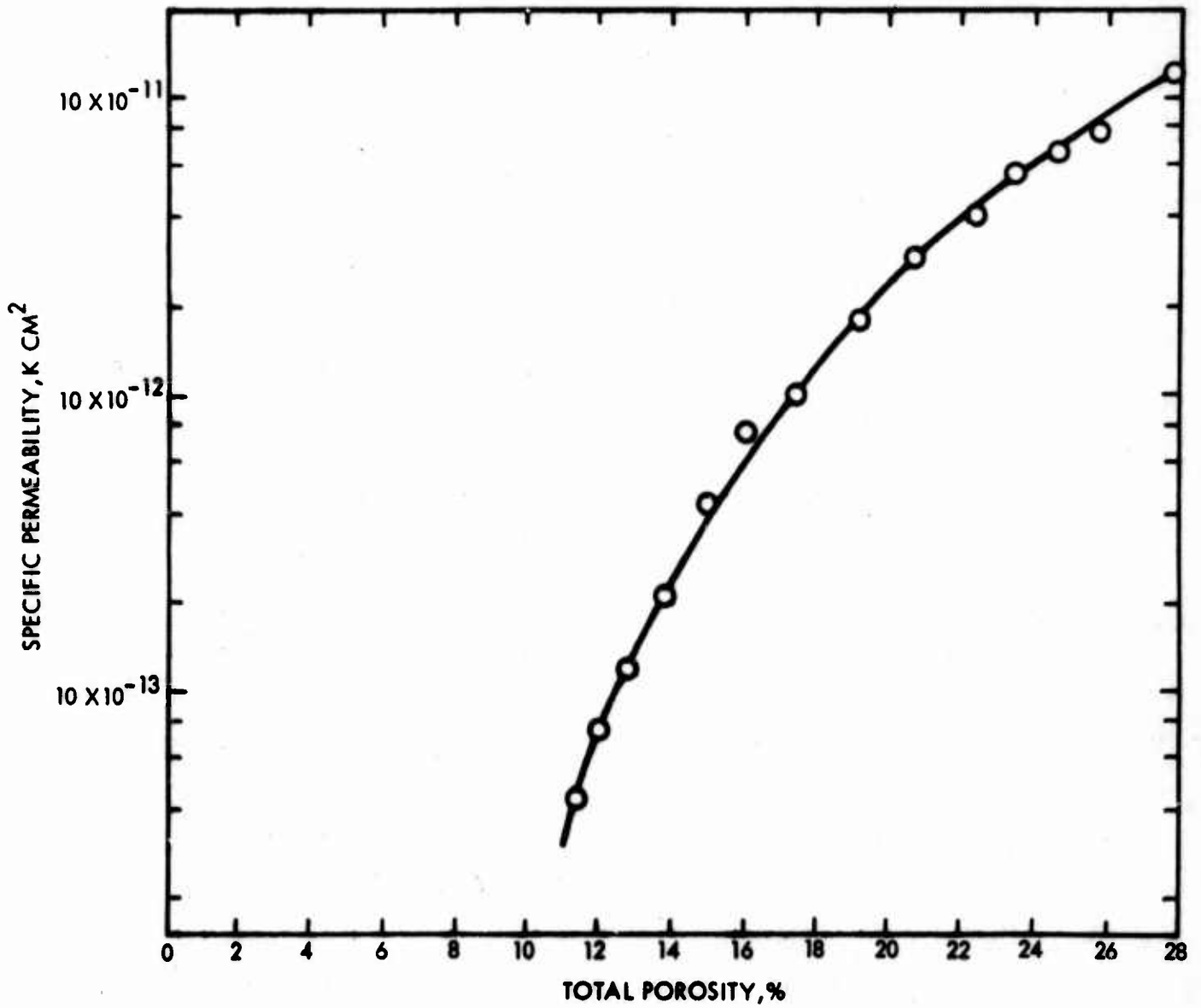


Figure 19. Relationship Between Porosity and Specific Permeability for Powder Lot UC-3.

diameter rhenium feed tubes. All joining was accomplished by vacuum brazing using a molybdenum-rhodium eutectic alloy.

After fabrication and brazing operation had been completed, the major face of the modules were Eloxed to form the fluted ion trajectory control surface. Figure 20 is a photograph of the ionizer module used in this program.

After the Eloxing, the modules are vacuum cleaned and electropolished to remove the as-Eloxed surface. Figures 21 and 22 show the contrast between the as-Eloxed surface and the surface after electropolishing. It can be seen from these figures that the electropolished surface is comparable to that of the parent materials, while the Eloxed surface has very little resemblance to the original porous tungsten surface. Pretest analysis was performed on all of the ionizer test buttons and consisted of the following:

1) Density

The density of all test buttons was determined using mercury emersion techniques. In each ionizer module, buttons of different densities were tested to provide a direct comparison of ionizer efficiencies at different densities.

2) Metallographic Analysis

Prior to assembly, each of the buttons was metallographically examined to provide information as to the uniformity of the porous network and the size and number of pores present. Photomicrographs similar to Figures 13 through 18 as shown earlier in this report were obtained and pore count data was taken using the previously-mentioned direct count method.

3) Permeability Tests

Permeability tests were taken on each of the test samples after all fabrication including Eloxing had been completed.

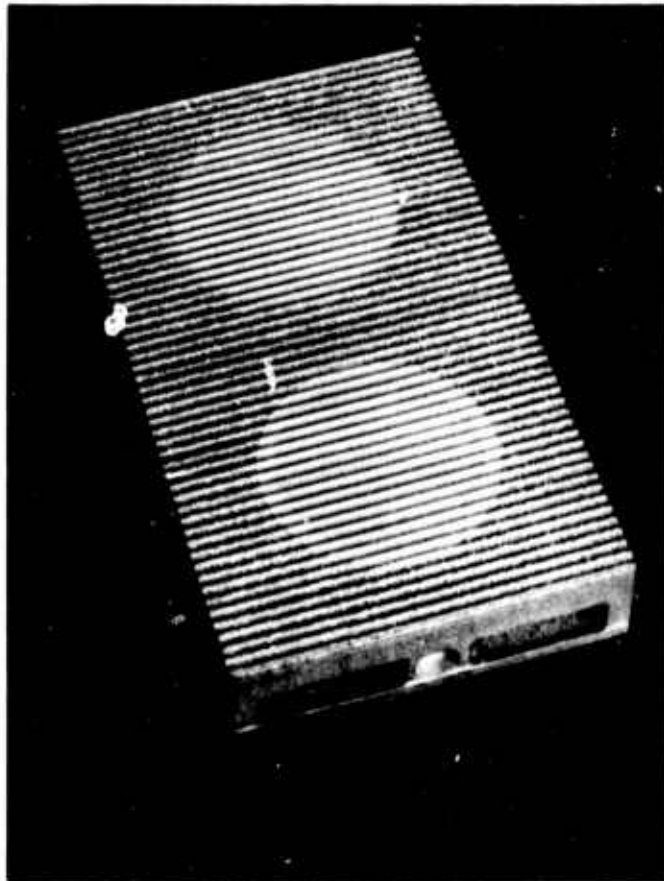


Figure 20. An Overall View of the Ion Emitter Module Used During This Program.

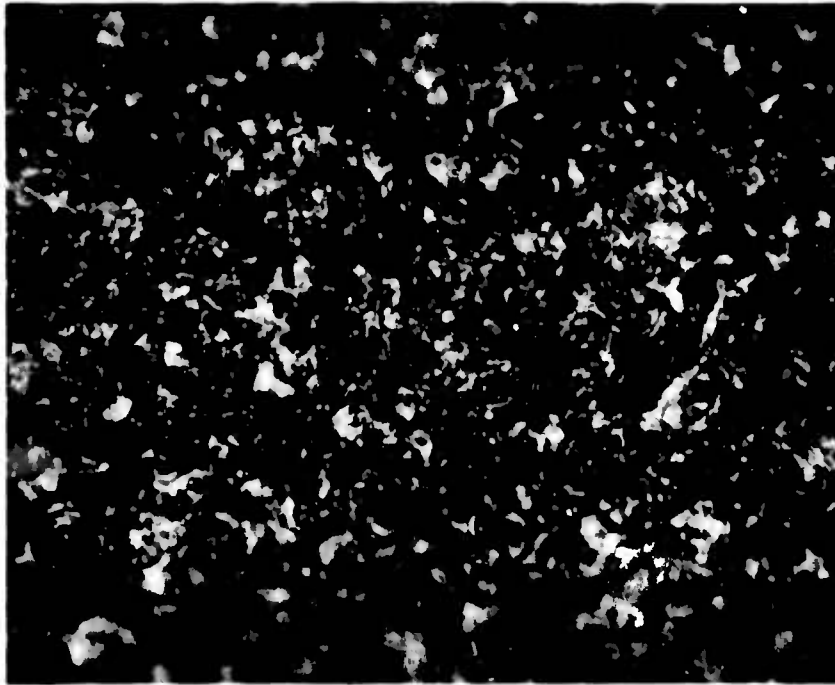


Figure 21. Surface of Ionizer After Eloxing.

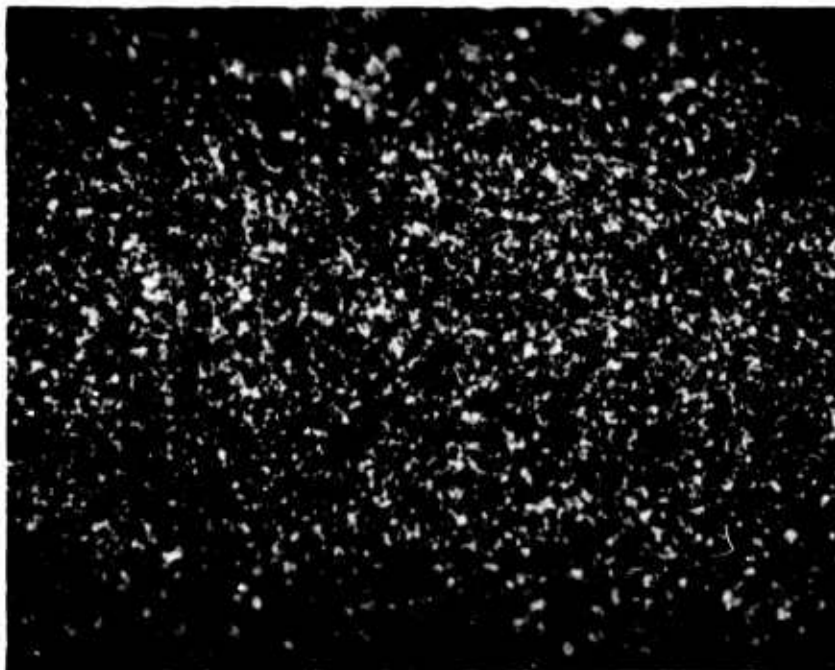


Figure 22. Surface of Ionizer After Eloxing and Electropolishing.

b. Ionizer Test Objectives

The objective of the ionizer tests is to obtain operational data on the performance of the ionizer under conditions representative of an ionizer engine. The selection of the test configuration was determined by several basic considerations. One of these was the choice of current densities that would be used during the tests and, for the fullest emitter evaluation, data should be obtained over as wide a range as possible. Extrapolation from lower current densities is often misleading and unreliable. Test configurations should provide for direct observation to as high a value as possible while the ionizer still maintains characteristics which are useful for engine application. The configuration that was selected and described in detail in the previous section was the design most compatible with all of the various conditions that are imposed on a test button. The advantages of this button type engine are as follows:

- 1) High current densities are readily obtainable because of the small spacing between emitter and grid.
- 2) Each pair of samples may be compared with a minimum of variation in operating conditions.

c. Test Procedures

The basic testing procedure was to measure the neutral cesium fraction from the emitter as a function of emitter temperature at selected values of ion current density. The neutral fraction was determined from beam-on versus beam-off readings taken from neutral cesium detectors collimated to cover the sample area. Emitter temperature was determined from a platinum-platinum 10 percent rhodium thermocouple attached to the solid tungsten portion of the emitter assembly.

In the actual tests, it was generally found that the emitter characteristics varied with time indicating changing surface conditions. In addition, some surface changes were made by the addition of either oxygen or acetylene. These gaseous additions were made in an attempt to clean the surface of the ionizer.

d. Test Results

The ionizer performance data for the six individual test samples are shown as Figures 23 through 28. Ion current densities to 32 ma/cm^2 were investigated on those specimens where possible. The FM-1 powder lot material produced ionizer data typical of metallic tungsten and exhibited a work function in the range of 4.6 to 4.8 ev. Porous material prepared from powder lot FM-2 exhibited a surface work function in excess of 5.0 ev and, therefore, it must be concluded that some contaminant was present in this material to produce this higher-than-normal work function. Both oxides and carbides of tungsten can produce this result. Analysis of these surfaces during ionizer operation revealed that carbides of tungsten were probably responsible for the observed behavior.

The data for ionizers prepared from UC-3 powders reveal typical performance data as a function of both temperature and ion current density. The data from the Union Carbide powder, buttons UC 3-5, is shown as a dashed line and only represents a relative value of neutral fraction versus a known temperature. This resulted from a neutral detector malfunction in the open position making accurate neutral determinations impossible. Data at high current densities on this button could not be obtained.

The overall results of the present ionizer evaluation testing confirm that the powders used during this development effort to prepare porous materials result in high performance ionizers. It would appear from these data when combined with previous ionizer performance data that original powder size, pore size, pore density, and other pore parameters are less important than the microscopic uniformity of these properties. Therefore, it is believed that the single most important property of an ionizer material is uniformity of permeability and porosity parameters.

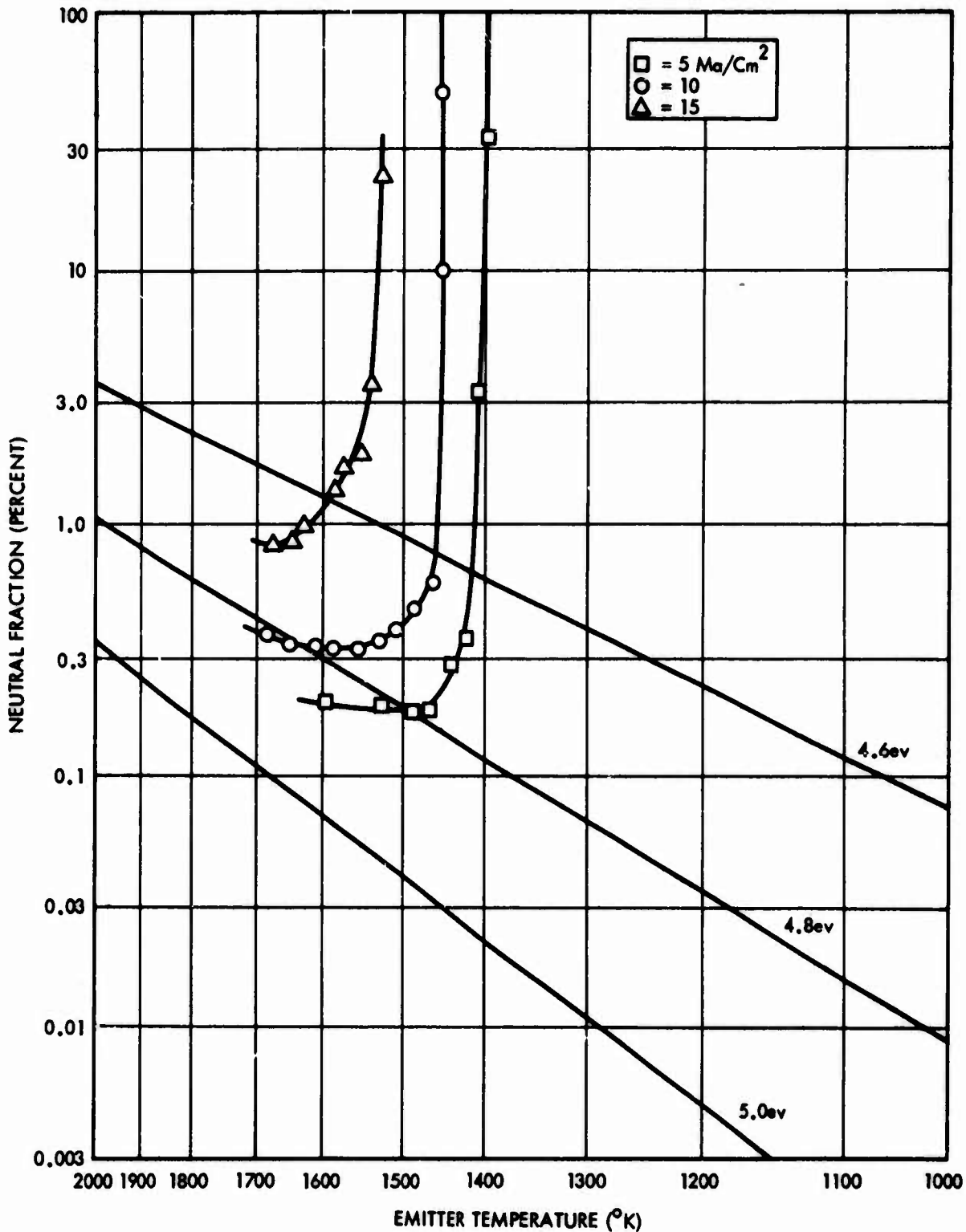


Figure 23. The Relationship Between Cesium Neutral Fraction as Percent Neutrals Versus Emitter Temperature in Degrees K for the Ionizer Compact FM 1-3.

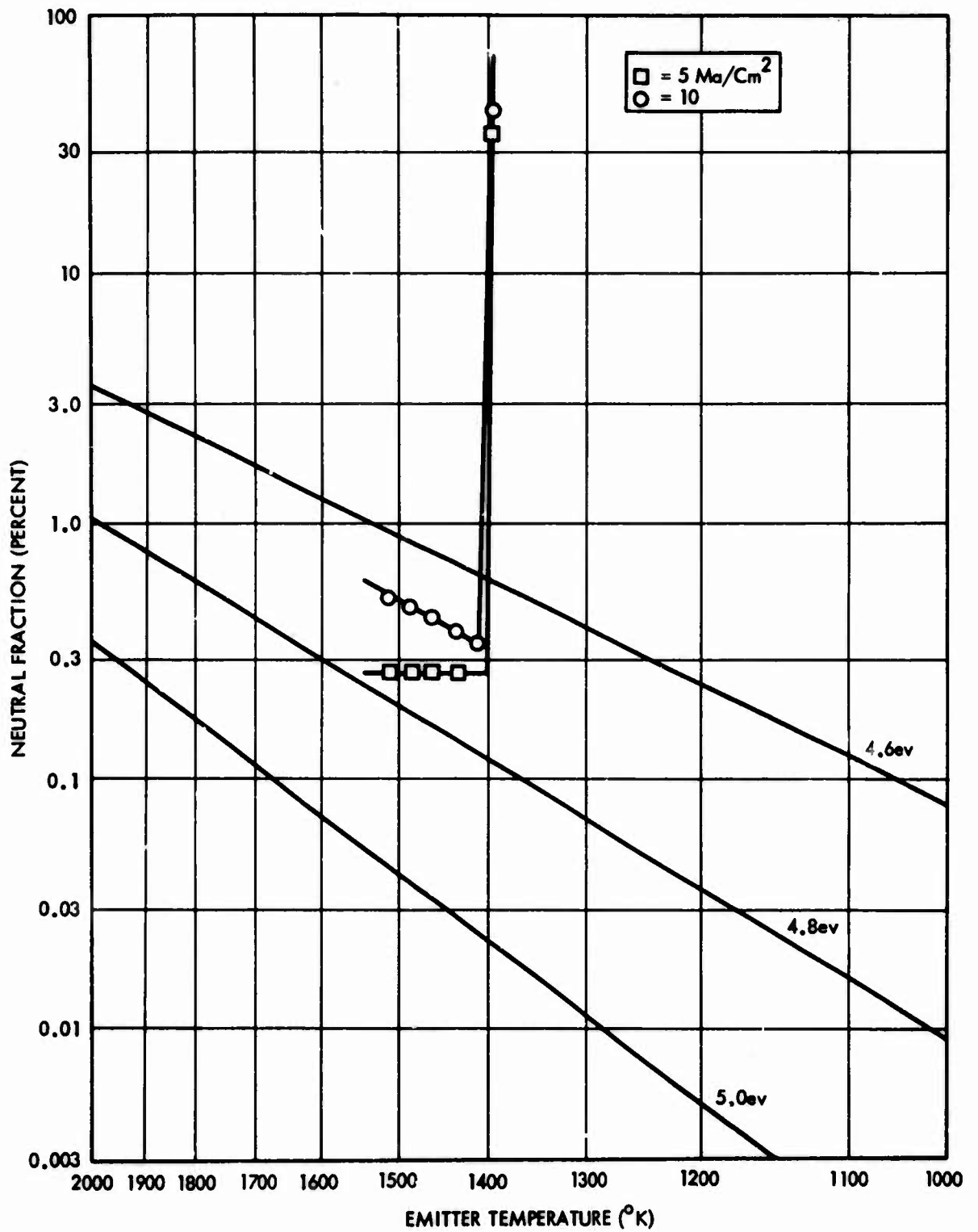


Figure 25. The Relationship Between Cesium Neutral Fraction as Percent Neutrals Versus Emitter Temperature in Degrees K for the Ionizer Compact FM 1-4.

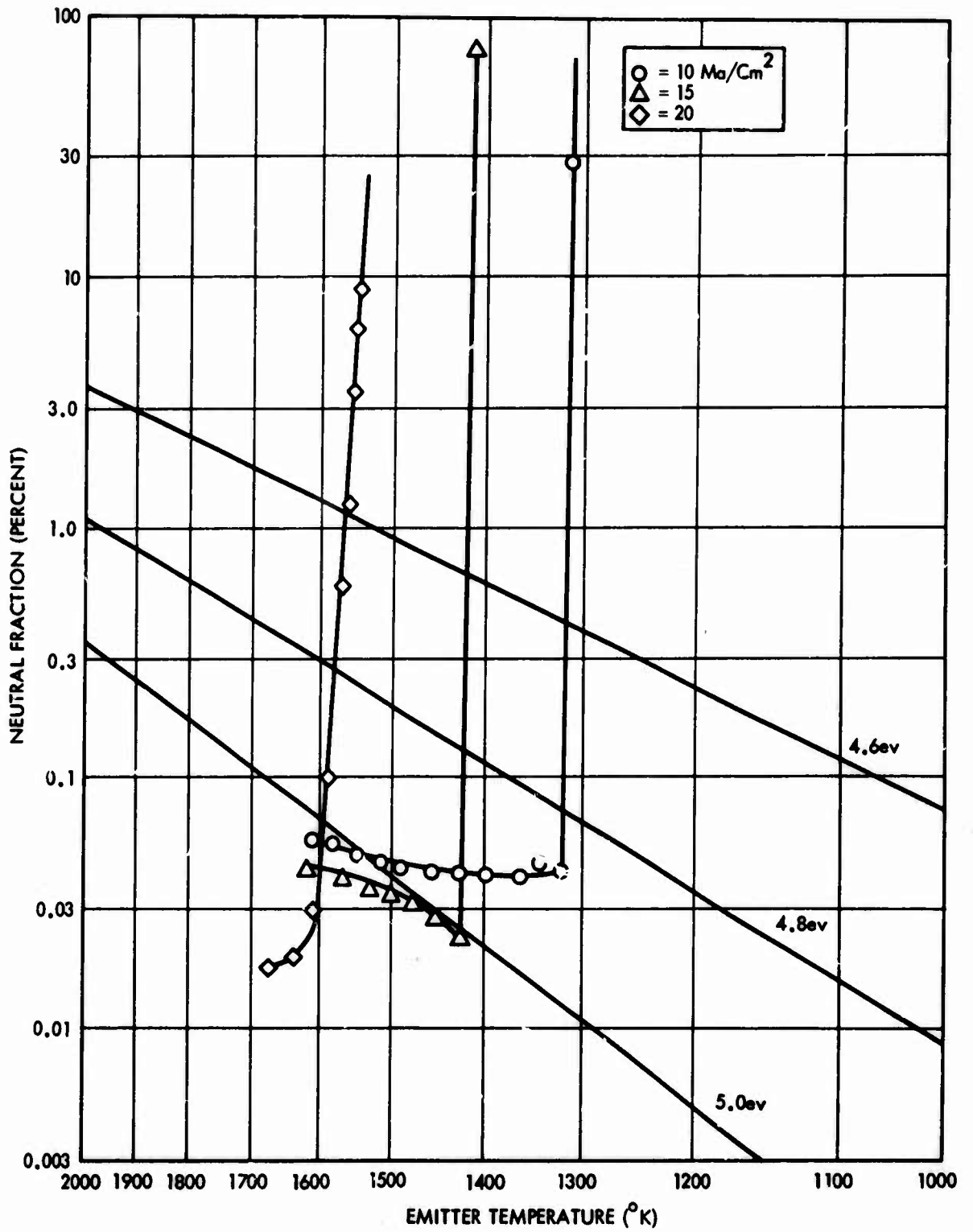


Figure 25. The Relationship Between Cesium Neutral Fraction as Percent Neutrals Versus Emitter Temperature in Degrees K for the Ionizer Compact FM 2-1.

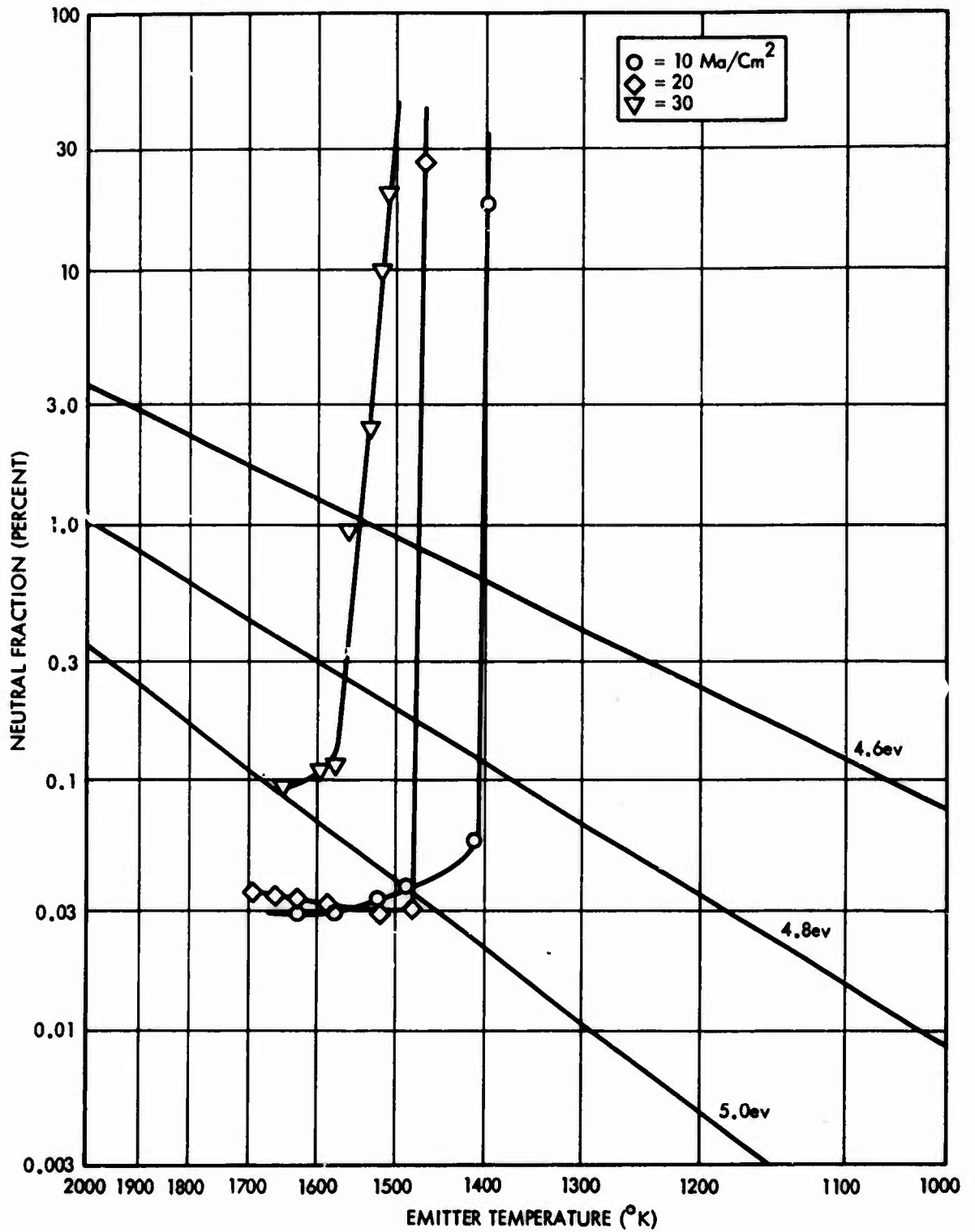


Figure 26. The relationship Between Cesium Neutral Fraction as Percent Neutrals Versus Emitter Temperature in Degrees K for the Ionizer Compact FM 2-2.

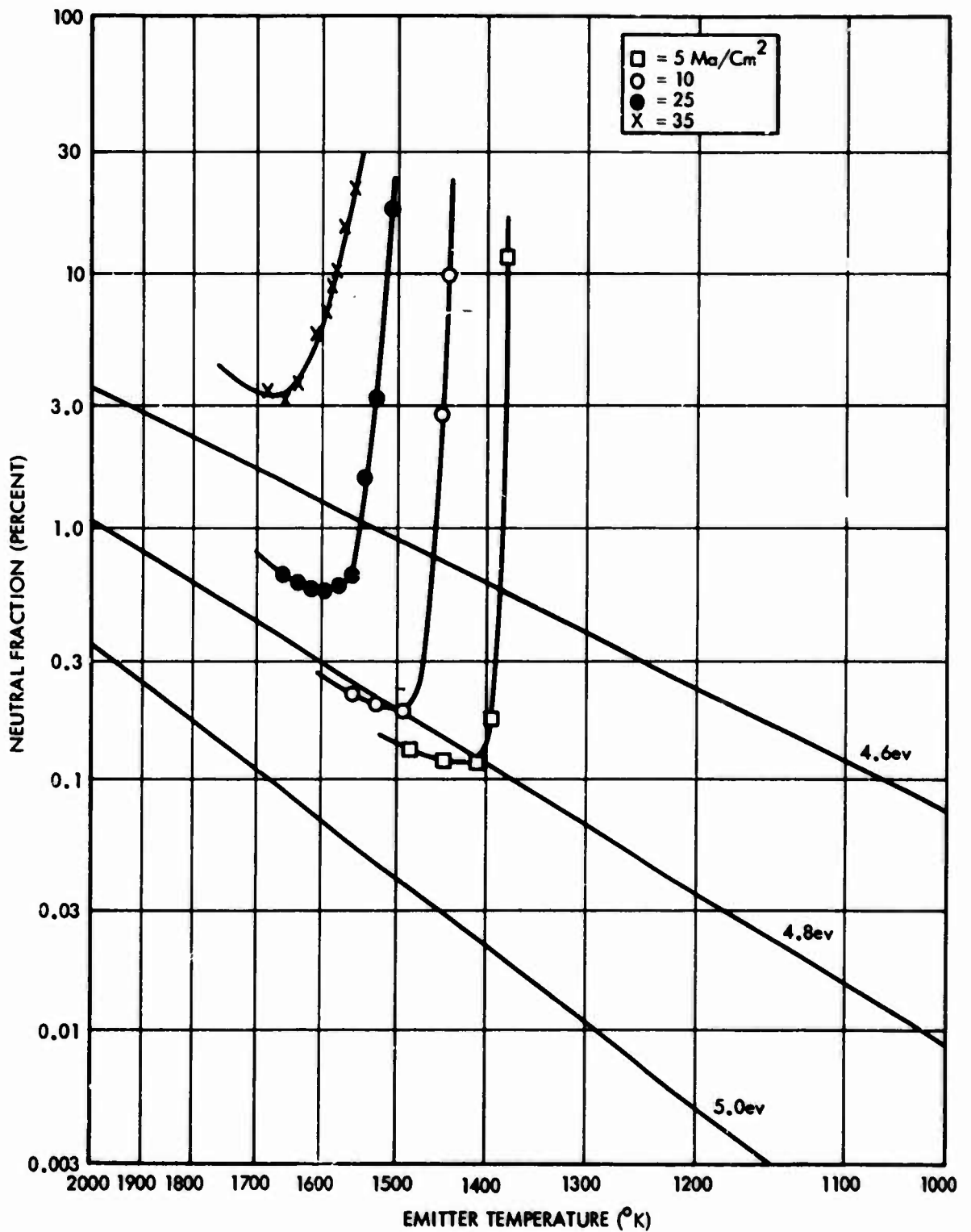


Figure 27. The relationship Between Cesium Neutral Fraction as Percent Neutrals Versus Emitter Temperature in Degrees K for the Ionizer Compact UC 3-8.

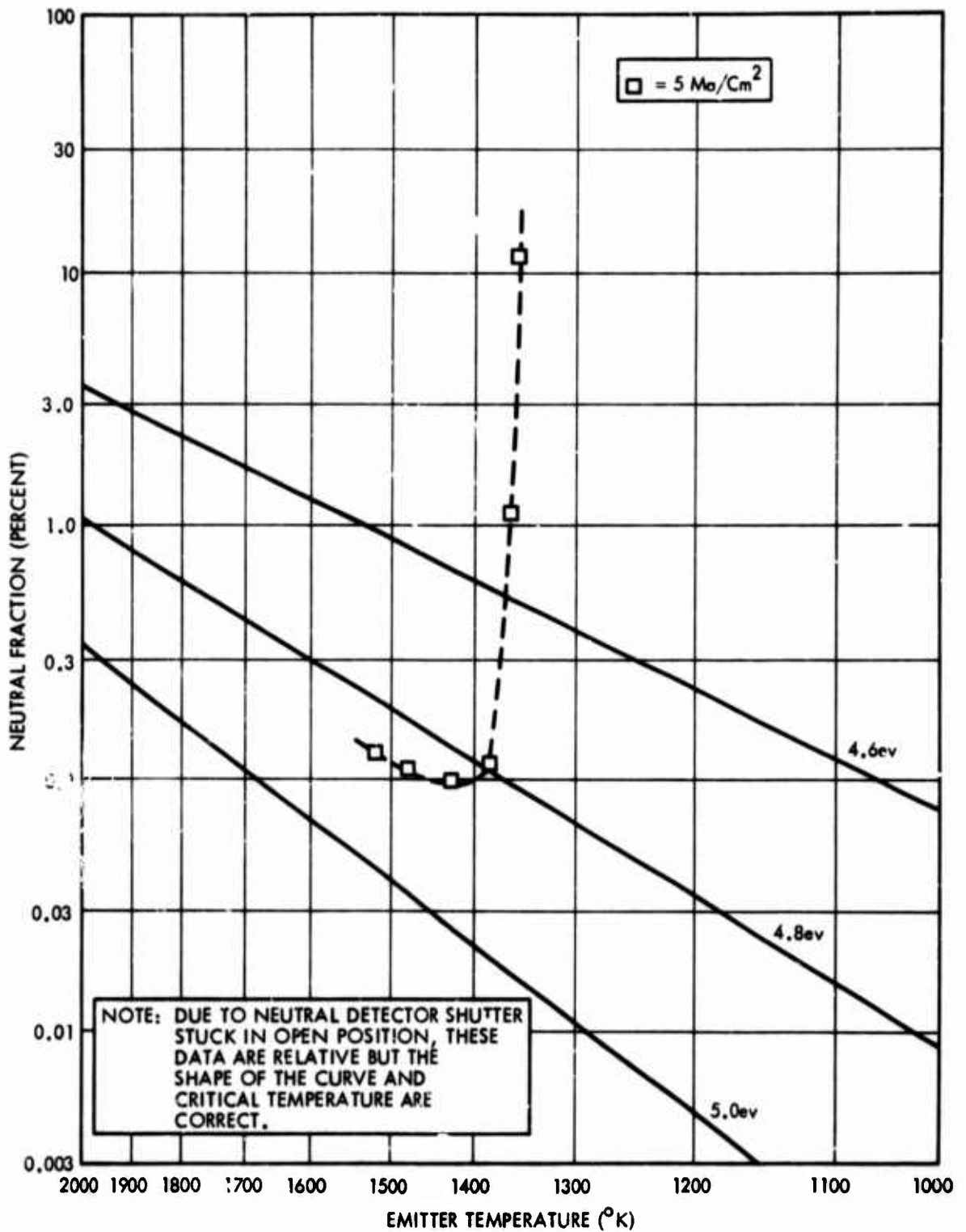


Figure 28. The Relationship Between Cesium Neutral Fraction as Percent Neutrals Versus Emitter Temperature in Degrees K for the Ionizer Compact UC 3-5.

4. Thermal Stability

Since a porous ionizer material must operate at elevated temperatures in the range of 1300° to 1600° K to efficiently produce cesium ions, the stability of the porous material is important if the ionizer is to operate for extended periods of time. Further sintering or densification of the ionizer material during its operation will reduce the surface pore density, porosity, and permeability and will result in decreased ionizer performance.

Long-term dimensional stability tests have been carried out in both vacuum and cesium environments for several types of porous materials. Figure 29 relates the log of time required to produce a 50 percent reduction in permeability as a function of reciprocal temperature. This figure was constructed using the stability test data obtained during this program in conjunction with Figure 19 which shows the decrease in permeability with increasing density. Using this combination of data, valid extrapolation can be made from density data. One caution that should be recognized in extrapolation of stability data to long times (10,000 hours) from short time data (200 hours) can be demonstrated in the following discussion.

The sintering of porous tungsten at high temperatures will follow a densification curve similar to those determined in the previous program as shown in Figure 30. This figure shows a rapid increase in density during the initial phases with a much lower increase during the later phases of sintering. It has been shown⁽⁸⁾ that it is impossible to obtain full densification of powder compacts by sintering alone without working and subsequent resintering. In the case of the stability tests which are conducted at a lower temperature after the tungsten has been reworked (machined into test configuration), it may be assumed that a similar rapid densification is present during initial resintering. This is followed by a slower rate of densification during the later stages of resintering. This is illustrated semi-qualitatively as Figure 31. Thus, if

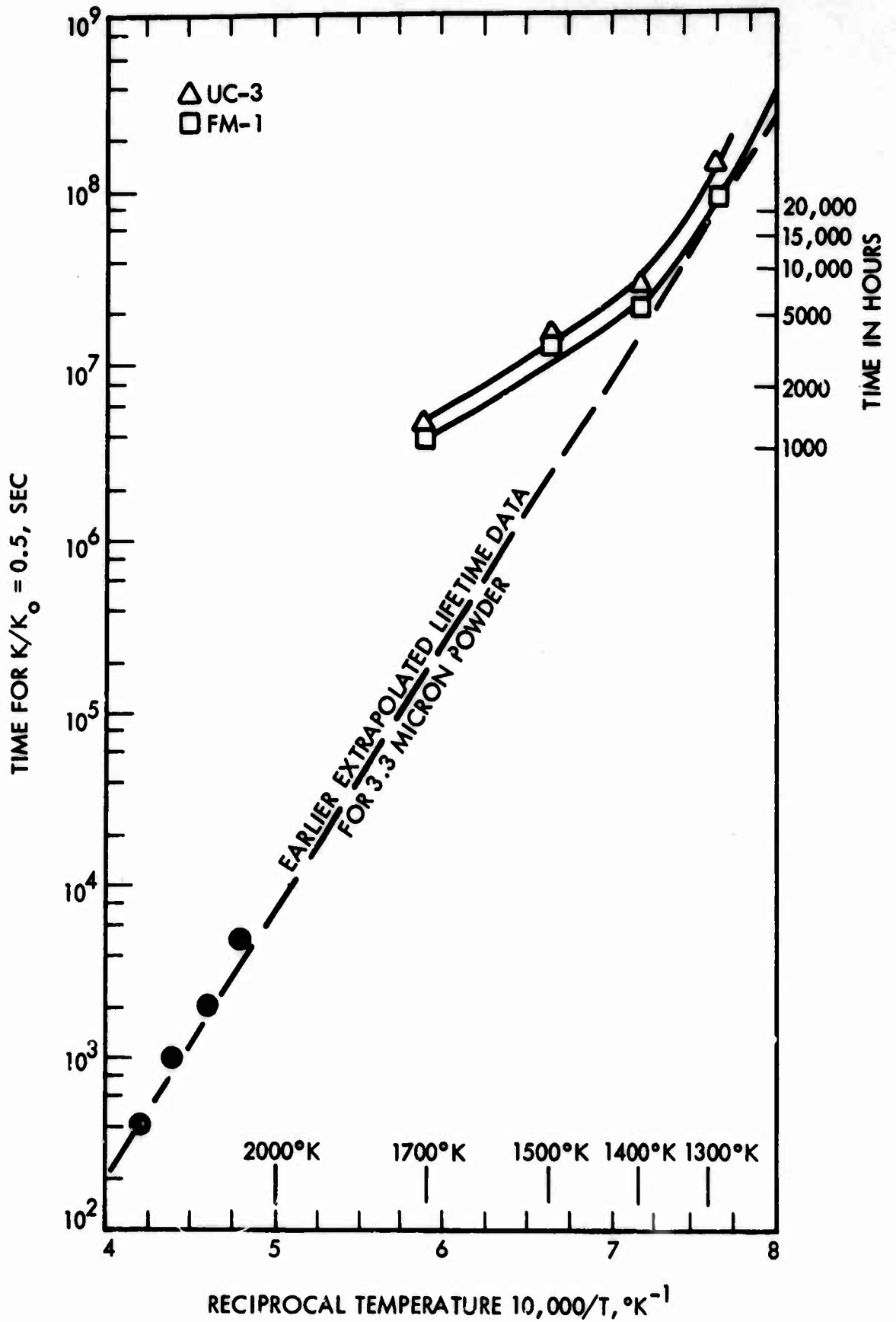


Figure 29. Relationship Between Ionizer Lifetimes and Temperature for Powder Lots FM-1 and UC-3.

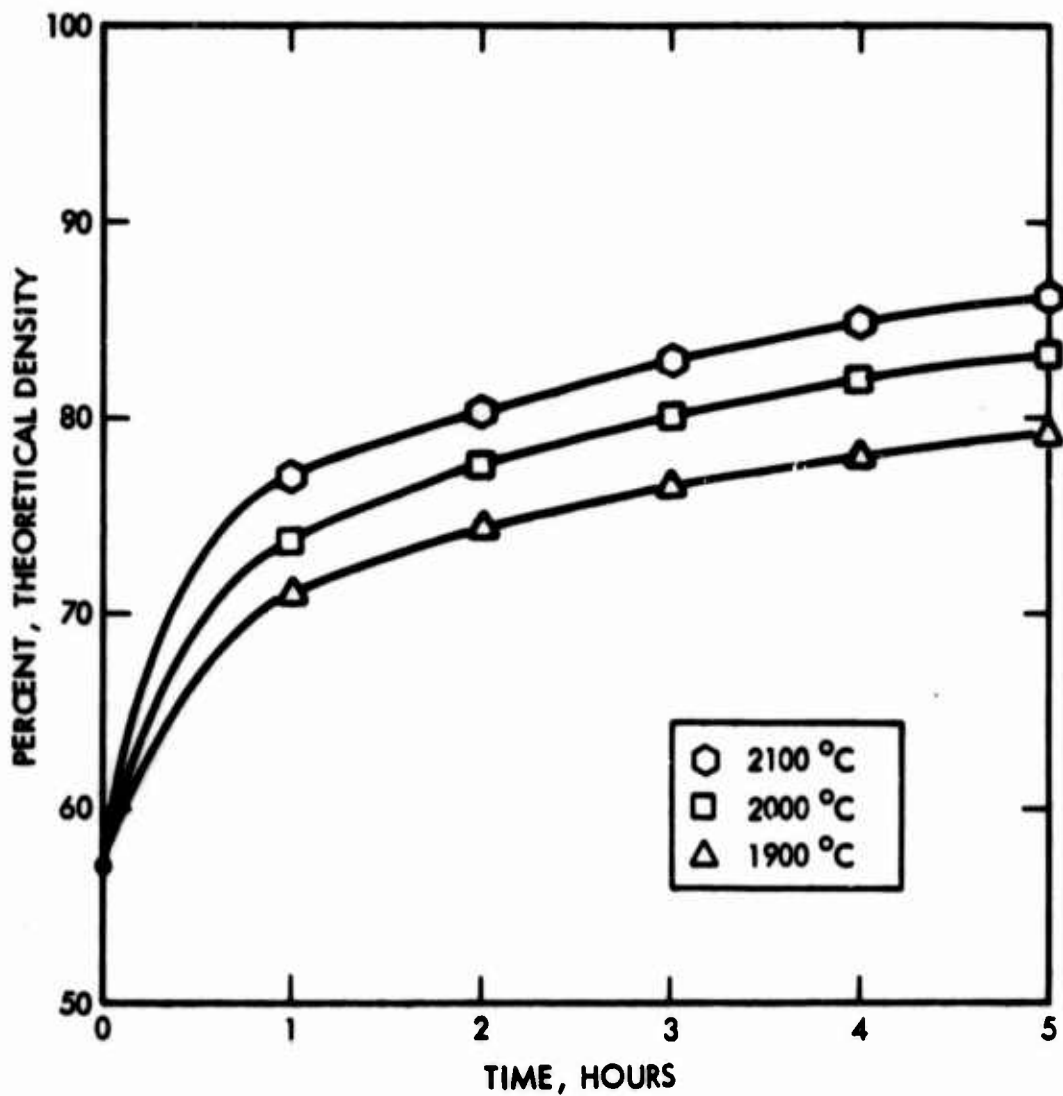


Figure 30. Densification Curve for a 6.9 Micron Powder Showing a Rapid Increase in Density During the Early Stages of Sintering.

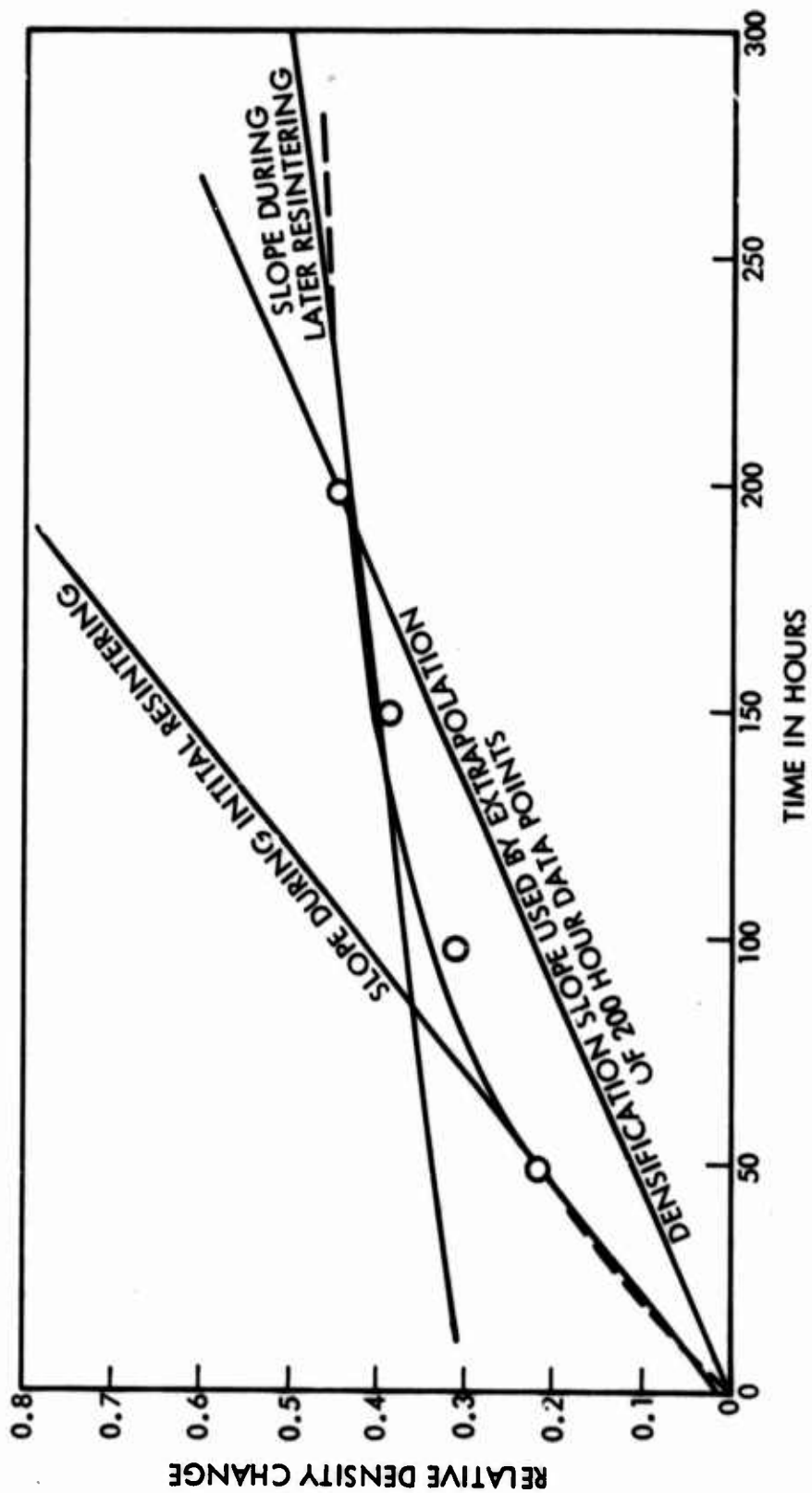


Figure 31. Densification Curve for Powder Lot FM-1 at 1700° K Showing A Rapid Increase in Density During the Early Resintering and a Lower Rate of Densification in the Later Resintering.

the slope of the sintering curve at the lower temperature is taken during the initial period, the time at which densification is rapid, conservative results will be obtained with regard to the lifetimes of the porous body. Although 200 hours is in fact a "long" time compared to the three or four hours required to sinter the tungsten initially, it should be noted that a different mode of sintering is taking place.⁽⁹⁾

A complete set of 200 hour data are presented in Table IX. These data were taken at 1300° K and show a slight increase in density. Other data taken at 1400, 1500, and 1700° K in four 50-hour runs are also presented.

The vacuum tests were performed in a tube furnace at a pressure of less than 10^{-5} torr except during heat-up when the pressure rose to approximately 5×10^{-4} . Since no sintering atmosphere, even vacuum, is ever free of oxygen or water vapor⁽¹⁰⁾ there is the possibility of oxidation of the tungsten even at a pressure of 10^{-5} torr. The oxidation of tungsten by water vapor is a continuous operation in that the oxide that is formed is volatilized off the tungsten surface. The oxide then decomposes into tungsten plus water vapor to repeat the cycle. In the case of the lower temperatures, the tungsten lost through oxidation may appear to decrease the density. However, there is an increase in density due to additional sintering.

Cesium stability tests were performed on an ionizer module following the ionization investigation. The engine module was run at temperatures from 1400° to 1700° K with current densities of 5 to 40 ma/cm² for the first 100 hours. During the second 100 hours, the emitter temperature was held at 1500° K, and the current density was held at 25 ma/cm². Permeability measurements taken before and after the ionizer had completed 200 hours revealed that there was no decrease in permeability. In all of the post-analyses of the ionizer modules where the porous tungsten is restrained, no decrease in

Table IX

Relative Density Change for Vacuum Stability
Samples After 200 Hours at 50-Hour Intervals¹

<u>Temperature</u>	<u>Powder Lots</u>		
	<u>FM-1</u>	<u>FM-2</u>	<u>UC-3</u>
1300°K	.02		.036
1300°K ²	.03	.01	.04
1400°K	.08		.14
1500°K	.16		.19
1700°K	.50		.58

1) data corrected for weight loss

2) 200-hour continuous test

permeability was noted after 100 hours at temperatures up to 1700° K and current densities from 5 to 40 ma/cm². The resistance to further sintering in the restrained case has been noted by other investigations.⁽¹¹⁾

The results of all of the stability data obtained during this program in conjunction with the data obtained during the earlier program indicate that pure spherical tungsten in the size ranges of four to five microns will provide lifetimes exceeding 10,000 hours.

IV. DISCUSSION AND REVIEW

The need for long-lived, low-thrust space propulsion engines for a variety of future planetary missions has prompted the development of contact-type ion engine systems over the past several years. This type of ion engine system makes use of a high temperature porous material as the ionizer and, thus, these systems have provided the impetus for the development of high performance porous tungsten materials.

In order to achieve the properties essential for high performance operation, a great deal of powder metallurgy development has been required. The desired properties of porous ionizers include uniform pore size, uniform pore spacing, surface pore densities approaching 10 million pores/cm², high temperature dimensional stability for periods of 10,000 hours, and a high electronic work function. In an effort to meet the latter two requirements, tungsten has received the most development attention. To meet the desired porosity and permeability requirements, uniformly-sized spherical powders have been employed. As a result, significant advances have been realized in the performance of ionizer materials during the past several years.

Spherical tungsten powders were selected for use in an effort to maximize size uniformity of powder particles within each powder lot. High purity tungsten powders were obtained which had been spheroidized by inert gas, plasma-arc techniques. All powders were then classified using a Cyclonic air classifier. A total of nine separate powder lots ranging in average particle size from 3.3 microns to 6.9 microns have been investigated during the course of these development programs. The typical purity of the starting spheroidized and classified powder is given in Table X. The purity level was also checked at various points throughout the processing sequence to insure against contamination during laboratory investigations. No significant impurity changes were observed during the course of this work. Table XI lists the powder lots investigated along with the average particle size and standard deviation for each powder.

Table X

Typical Impurity Levels of Tungsten Powders
As Determined By Spectrographic Analyses

<u>Element</u>	<u>Impurity Level PPM</u>
Ti	10*
Fe	10*
Cu	10
Ni	10*
Al	10*
Ca	20
Si	10*
Mn	10*
Cr	10*
Mg	10
Mo	10*
Total Other	300*

*Less than indicated amount

Table XI

Powder Parameters

<u>Powder Lot</u>	<u>Average Particle Diameter, Microns</u>	<u>Standard Deviation, Microns</u>
1	3.3	0.9
2	3.4	0.8
3	3.6	1.1
4	3.9	1.0
5	4.2	1.2
6	4.3	1.2
7	5.1	1.1
8	5.8	1.8
9	6.9	1.5

A semi-isostatic powder compaction technique was developed and used throughout the present investigations. This technique consisted of the use of a double die insert combination of elastomeric materials to isolate the powder compact from the die walls and to provide a load distribution medium to promote uniform compaction of the powder. Compaction was carried out using a conventional, double-acting punch and die assembly. Dow Corning DC 6510 silastic was used as one insert to totally enclose the powder. American Latex Daycollan 80 polyurethane was placed such that it totally enclosed the silastic insert and was in contact with all interior punch and die surfaces. The selection of elastomeric materials was based on property requirements at each of the interfaces of concern. Figure 32 is a cutaway sketch of the punch and die assembly. The size of "green" compacts prepared for evaluation was approximately 2.50" x 1.40" x 0.25".

Powell⁽¹²⁾ and others⁽¹³⁾ have investigated the use of single elastomeric insert materials to approach isostatic conditions within punch and die assemblies. Figure 33 shows a comparison of achieved "green" densities for single and double insert compaction versus conventional punch and die results for tungsten powders.

All powder compacts prepared during this investigation were sintered in a resistively-heated vacuum furnace. The furnace element consisted of 90 percent tantalum-10 percent tungsten sheet material which was fully enclosed with a tungsten sheet baffle to reduce line of sight paths between the tantalum furnace interior and the porous research material, thereby, minimizing metallic contamination during sintering. Preliminary sintering investigations were carried out using powder compacts having a size of approximately 1 cm x 1 cm x 0.3 cm. The detailed data concerning sintering rates as a function of temperature, compacting pressure, and particle size are the subject of a separate report.⁽¹⁾ Typical sintering data along with the resulting structure and properties for the porous ionizer materials developed are discussed below.

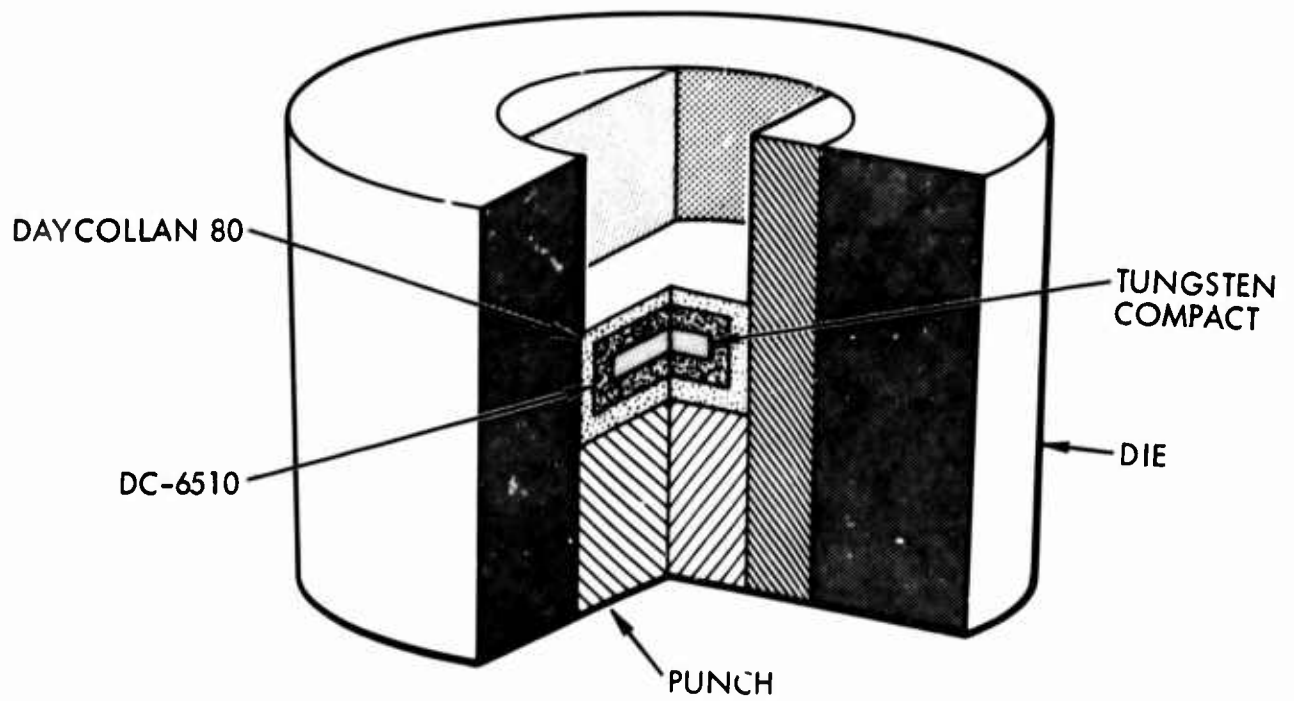


Figure 32. Cut-Away View of the Powder Compacting Die Showing the Double Insert Configuration.

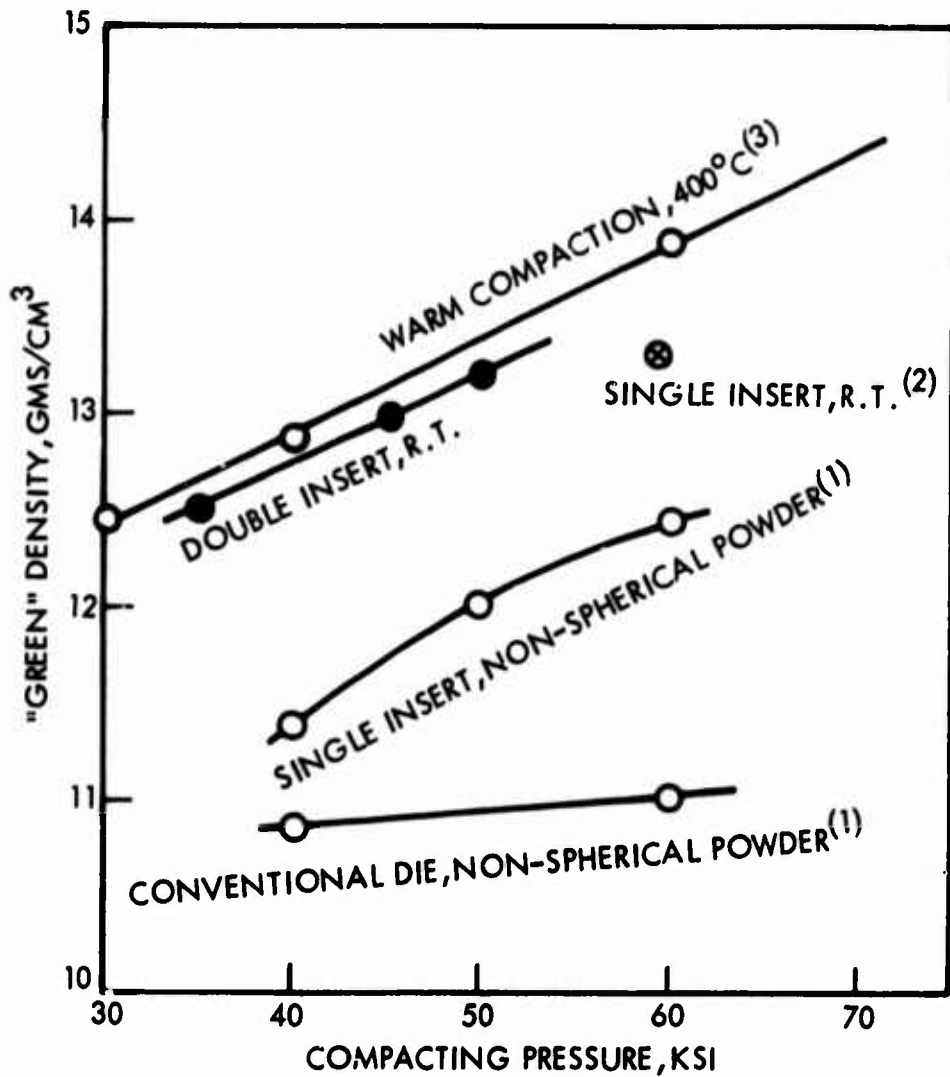


Figure 33. "Green" Density as a Function of Compacting Pressure for Various Types of Compaction Methods.

Typical sintering rate data are listed in Table XII for three separate powder lots investigated. It will be noted that these data represent average values for ten or more one square centimeter compacts studied during the preliminary phase of this work. It has been found that the larger compacts of interest for ionizer material require somewhat longer times or higher temperatures to achieve equivalent densities. Due to program limitations, comprehensive sintering rate data were not obtained for the larger compact types. Figure 34 is a plot of density data versus time for powder lot 3, which had an average particle size of 3.6 microns, for each of the four temperatures investigated.

In an attempt to correlate the effect of particle size on sintering rate, the Arrhenius plot of Figure 35 was constructed to show the relationship between sintering rate during the early stages of densification and reciprocal temperature for each of the three separate powder sizes. It will be noted that the slopes for each of these curves are similar and, therefore, each powder size has a similar activation energy. The relationship between sintering rate, again for the early stages of densification, and the reciprocal surface area of particles within the compact, is shown as Figure 36. These data thus provide the interrelationship between particle size, temperature, and time for the early stages of densification for spherical tungsten powders in this range of sizes.

The porosity of a material is defined as the total void volume per unit volume of material. Thus, one minus the fractional density provides the total porosity data. During this investigation, porosities ranging from 10 percent to 30 percent have been studied. Figure 37 is a photomicrograph of a sintered porous tungsten structure which has a total porosity of 25 percent. For a porous structure of this nature, studies have revealed that greater than 98 percent of the total porosity is interconnected. In all cases, the total starting porosity of ionizer materials was in the range between 20 and 30 percent, and where not otherwise specified, all reported pore parameter data are for porosities of 20 percent.

Table XII

Sintered Densities for Three Powder Lots Investigated

<u>Powder Lot</u>	<u>Sintering Temp. °C</u>	<u>Percent Theoretical Density*</u>				
		<u>Sintering Time, Hours</u>				
		<u>1</u>	<u>2</u>	<u>3</u>	<u>4</u>	<u>5</u>
3	1800° C	75.8	79.0	81.7	83.6	85.0
3	1900° C	78.9	82.3			
3	2000° C	83.4	85.7	86.8	87.8	88.5
3	2100° C	87.0	88.1	89.0	90.0	
7	1900° C	73.7	76.7	78.6	80.1	
7	2000° C	77.0	79.8			
7	2100° C	80.0				
9	1900° C	71.3	74.2	76.4	78.0	79.2
9	2000° C	73.7	77.6	80.1	81.9	83.1
9	2100° C	77.0	80.2	82.9	84.8	86.3

*Average values for ten or more one cm² compacts

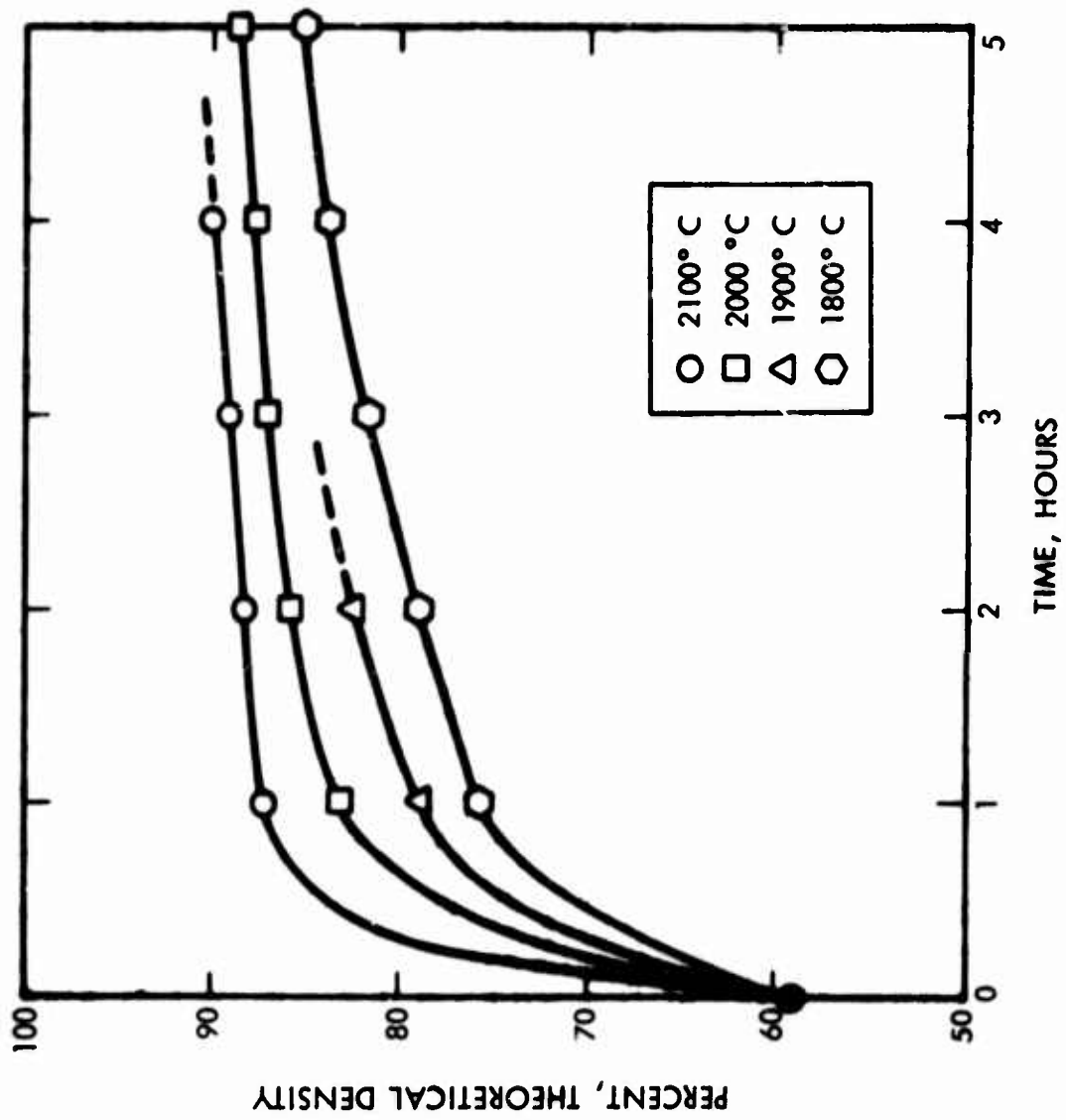


Figure 34. Sintering Rates at Various Temperatures for Powder Lot 3.

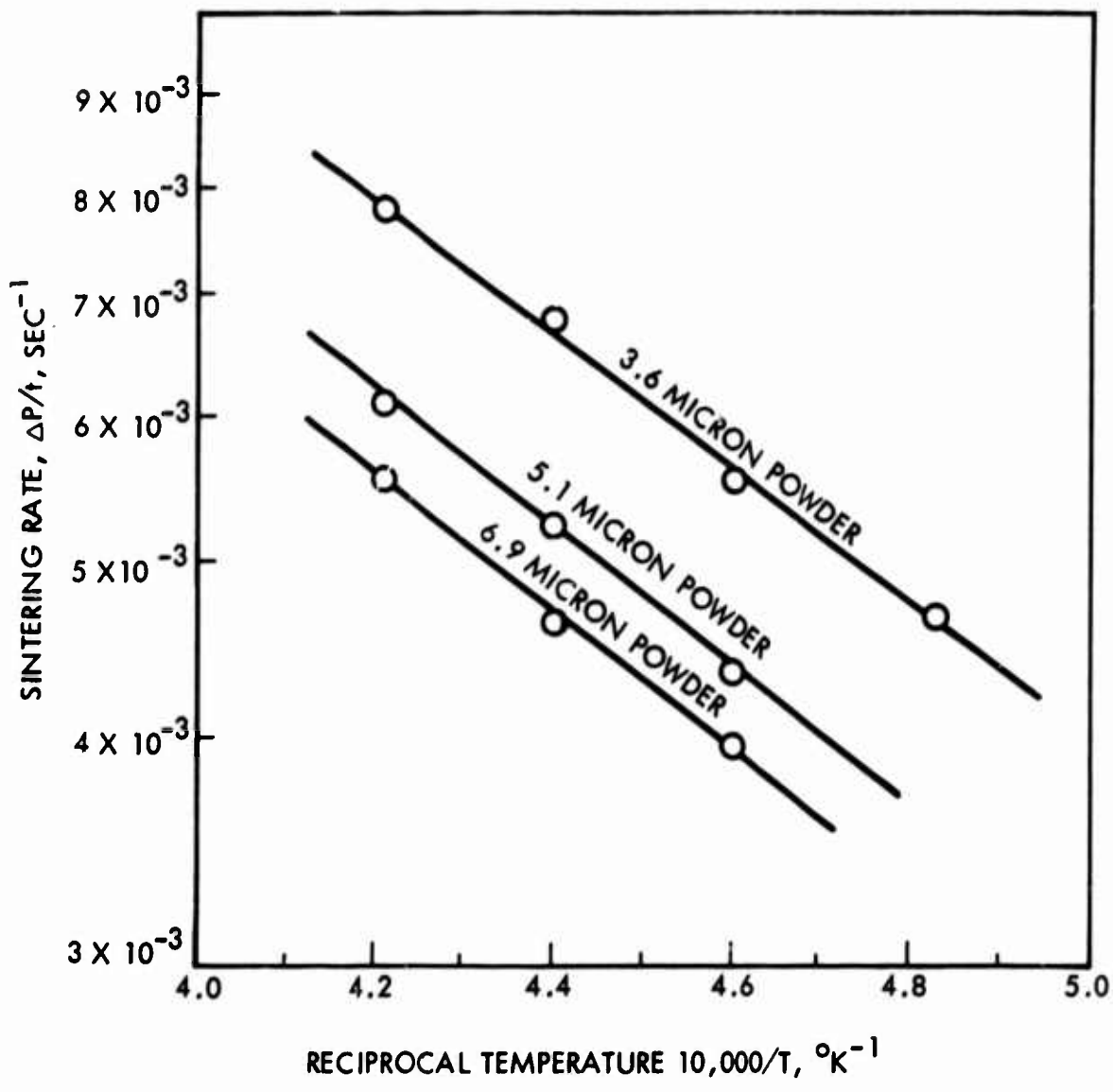


Figure 35. Arrhenius Plot of Sintering Rate for Powder Lots 3, 7, and 9.

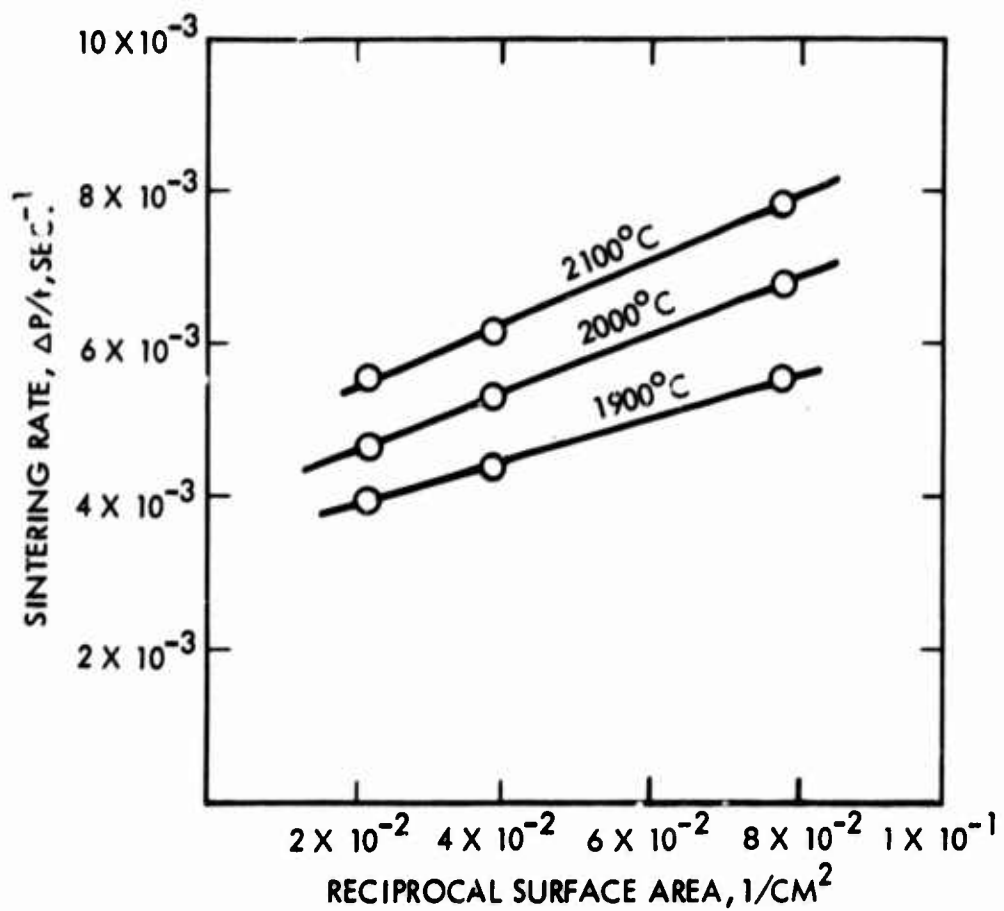


Figure 36. Relationship Between the Sintering Rate and Reciprocal Surface Area for the Temperatures Shown.

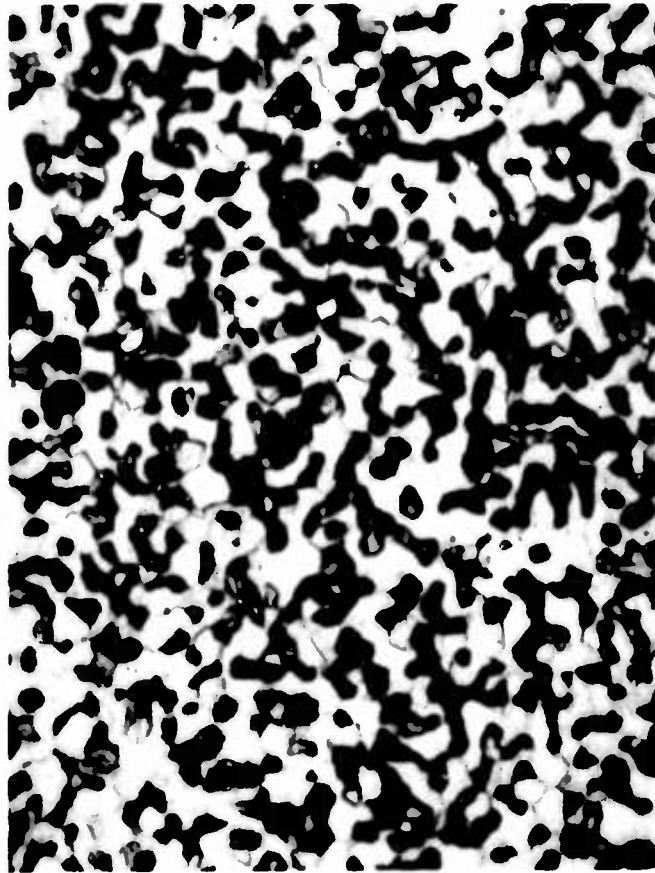


Figure 37. Typical Photomicrograph of a Porous Structure from Powder Lot 3. X1000

The porous material structural parameters of interest in ionizer applications include the average pore size, average pore spacing, and average surface pore density. The deviation within each of these parameters is also of interest since microscopic uniformity is of utmost importance for ionizer performance. Table XIII is a list of observed pore parameters for each of several powder lots studied during this investigation. It will be noted that the calculated values for the total pore area per unit of macroscopic surface area is in good agreement with the range of porosities for the specimens investigated. From these data, a number of generalized relationships can be derived between particle size and the several pore parameters of interest. Figure 38 shows this for surface pore density in comparison with calculated values for idealized packing of uniformly sized spheres, and in contrast to that observed for nonspherical powder materials. The larger deviations for smaller powder sizes, between the "ideal" curve and the observed data from the present studies, are believed primarily due to current inability to uniformly classify or size the smaller diameter powders.

The permeability measurements were based on gas flow data as a function of differential pressure. The basic relationship⁽⁷⁾ used was that for specific permeability, K, which is:

$$K = \frac{q\mu}{A(\Delta P/L)}$$

where: q = fluid flow rate
μ = fluid viscosity
A = cross-sectional area
ΔP = differential pressure
L = thickness

Table XIII

Porosity and Permeability Parameters for Several Types of Porous Materials Investigated

Total Porosity Range - 20 to 22%

<u>Powder Lot</u>	<u>Average Particle Diameter, μ</u>	<u>Average Surface Pore Density, $\times 10^6/cm^2$</u>	<u>Average Pore Diameter, μ</u>	<u>Total Pore Area cm^2 per cm^2</u>	<u>Specific Permeability $K cm^2$</u>
1	3.3	8.4 ± 0.4	1.8	0.21	3.0×10^{-11}
3	3.6	6.6 ± 0.5	1.9	0.19	4.6×10^{-11}
6	4.3	5.1 ± 0.5	2.2	0.19	4.9×10^{-11}
7	5.1	4.4 ± 0.3	2.4	0.20	5.7×10^{-11}
8	5.8	3.9 ± 0.3	2.7	0.22	7.0×10^{-11}
9	6.9	3.1 ± 0.3	3.0	0.22	---

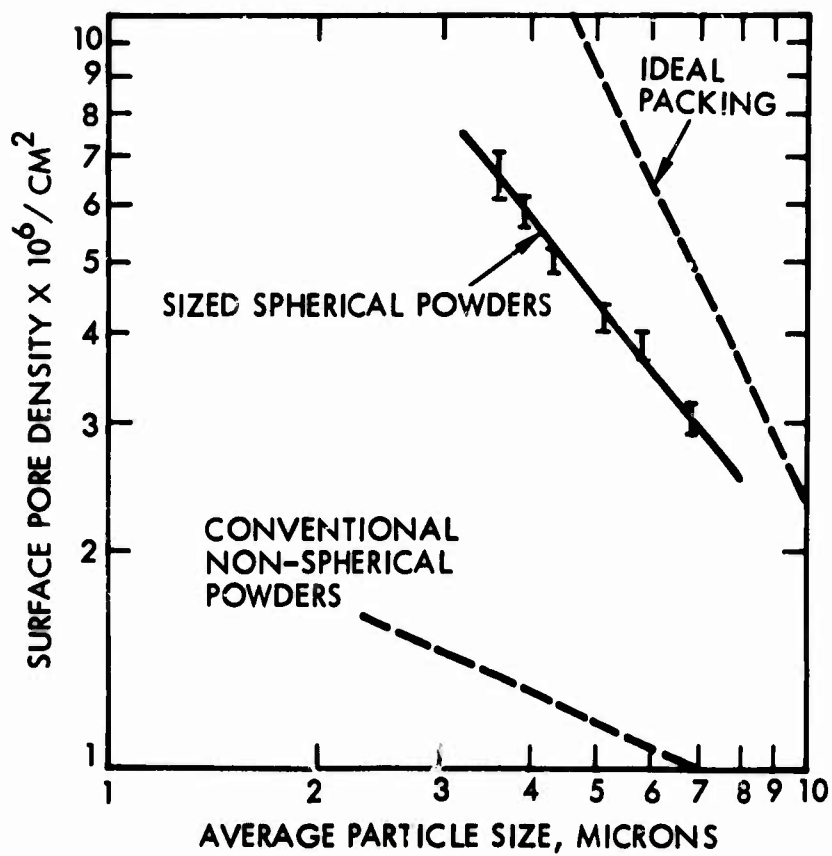


Figure 38. The Observed Surface Pore Densities as a Function of Particle Size Shown in Relation to (a) the Expected Values of Ideal Packing of Uniform Spheres Were Realized, and (b) the Typical Values for Non-Spherical Powder.

Dimensionally, the units of specific permeability are length squared, or area, and by accounting for the fluid viscosity, the magnitude of the specific permeability is independent of the nature of the flowing fluid over the range of interest.

The observed relationship between total porosity and specific permeability for porous material prepared from powder lot 3 (4.2 micron average particle size) is given as Figure 39. These data reveal a change of 2 1/2 orders of magnitude in specific permeability for a change in porosity of less than 20 percent. It will be noted from these data that pore separation or isolation has substantially reduced the permeability at porosities of approximately 10 percent.

The present investigations leading to the development of high performance ionizer materials have included a series of ionizer performance evaluations using an ionizer configuration similar to the TRW ion engine system.⁽¹⁵⁾ Porous tungsten ionizer test material was prepared and mounted within an emitter module as shown by Figure 40. The emitter surface area was 2.5 cm² which was believed to be large enough to represent the overall uniformity of the research material. Ionizer evaluation consisted of the determination of the cesium neutral fraction within the ion beam as a function of temperature over a range of ion current densities. Details of the ionizer module fabrication and test procedure are reported elsewhere.

The typical range of minimum neutral fraction as a function of ion current density is shown in Figure 41 for pure, spherical powder porous tungsten ionizer material prepared during this laboratory investigation. It will be noted that a substantial improvement in ionizer performance has been realized through the use of spherical powder in the preparation of ion emitter materials. Ionizer performance in the range of ion current densities investigated did not vary in a systematic manner with starting powder size or surface pore density. It would appear from the data of

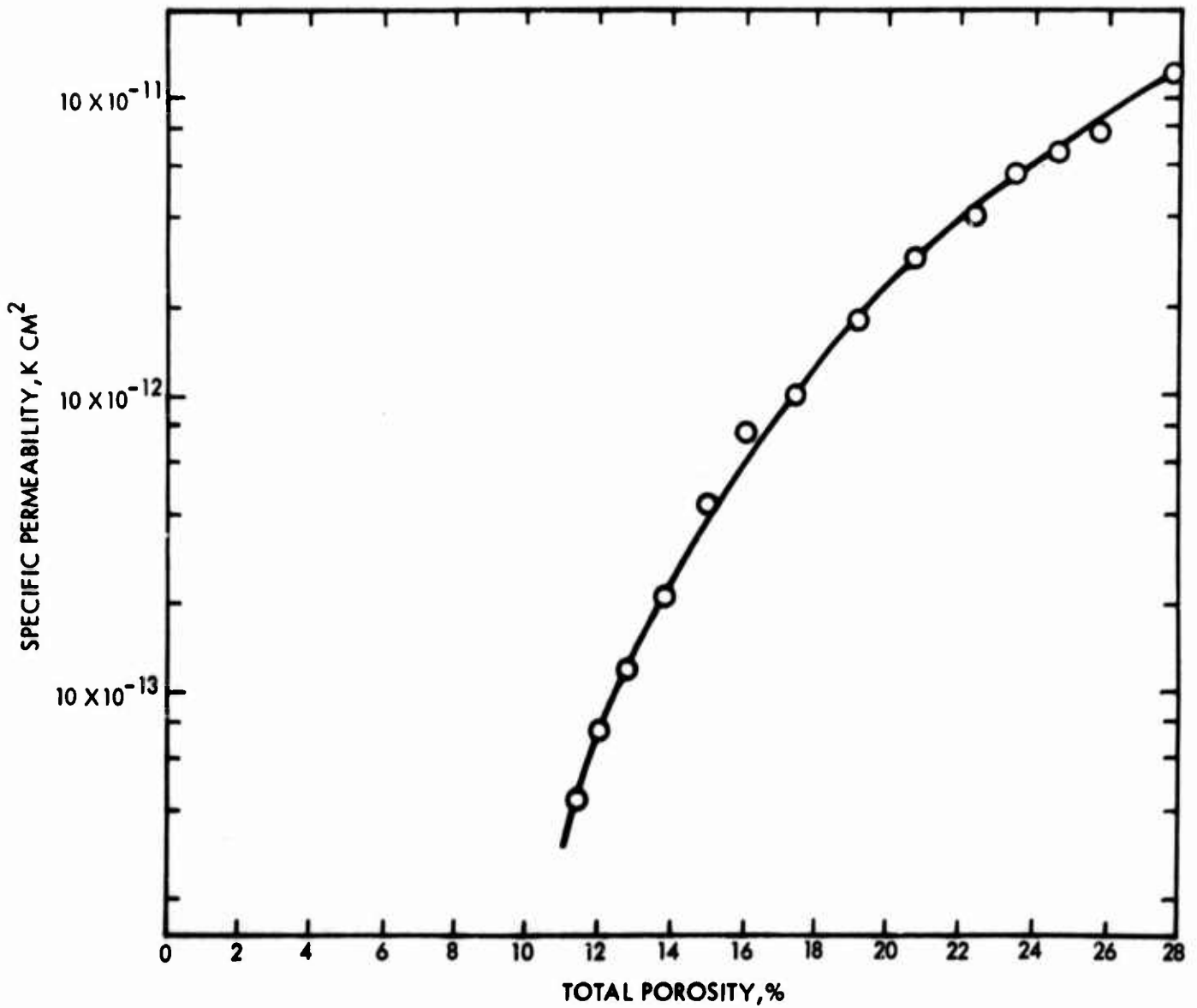


Figure 39. Relationship Between Porosity and Specific Permeability for Powder Lot 3.

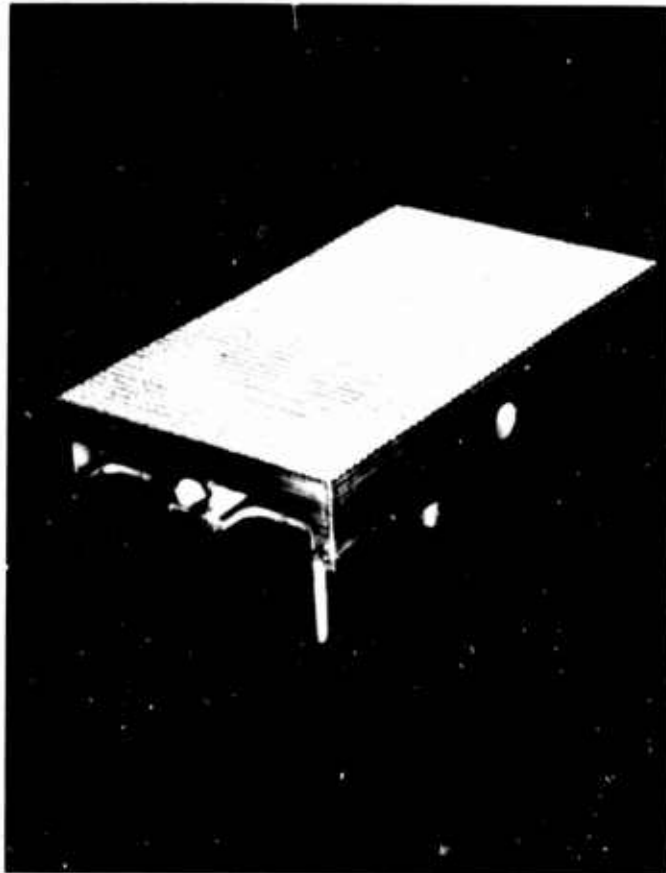


Figure 40. Photograph of an Emitter Module Used for Cesium Ionization Testing. The two Circular Areas on the Major Face are Separate Porous Tungsten Specimens Brazed into the Fully-Dense Tungsten Plenum Assembly.

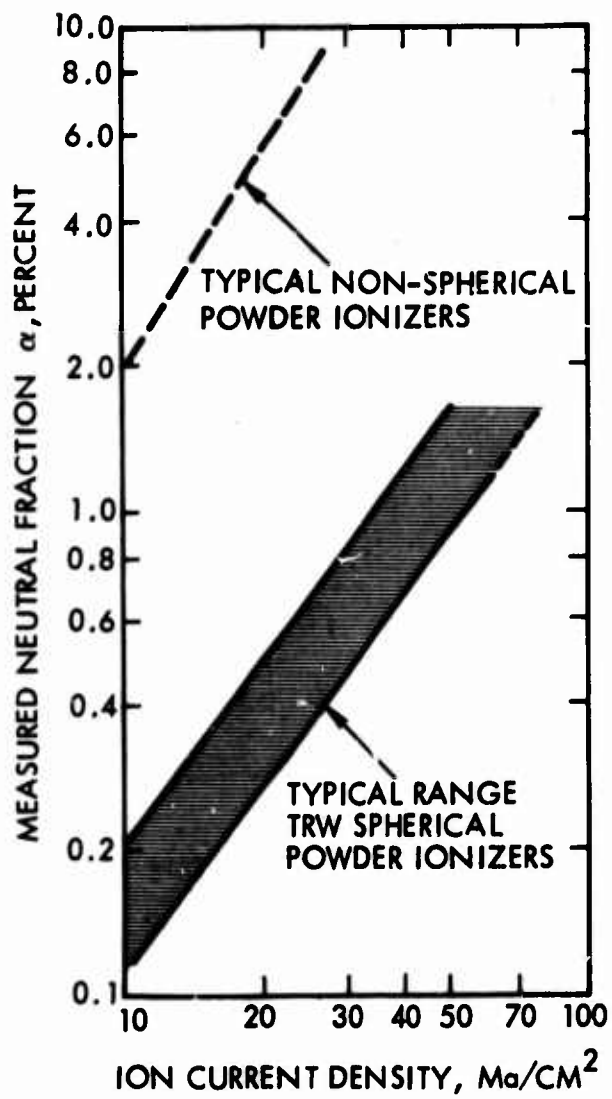


Figure 41. Observed Relationship Between Cesium Neutral Fraction and Ion Current Density for Spherical Tungsten Powder Ionizers Investigated.

this investigation that the most important benefit derived from the use of spherical powder particles is the greater uniformity in pore size, pore spacing, and permeability.

V. SUMMARY

It is clear from the data presented that significant gains have been realized in understanding and improving the structure and properties of porous ionizer materials. The use of spherical powder has resulted in numerous benefits which have led to the current high performance ion emitter materials. It would appear that future advances in ionizer performance await further research and development in the areas of:

1. Powder classification techniques
2. Spherical alloy powders
3. Low density, high porosity ionizers
4. Stable, high work function surface coatings

It is believed that ion propulsion systems will be important in the future exploration of our solar system. However, further development of ion propulsion materials and systems awaits the identification of specific missions and the development of suitable power sources.

REFERENCES

1. Kirkpatrick, M. E. and Mendelson, R. A., "Development of High Performance Porous Tungsten Ionizers," Technical Report AFML-TR-65-215, July 1965.
2. Turk, R. R. and McKee, W. E., "Ion Engine Supporting Research and Evaluation," Vol. I Materials Studies, Technical Report NASA CR-5441, November 1965.
3. Turk, R. R., Private Communication, June 1966.
4. LaChance, M., Thompson, B., Todd, H., and Kuskevics, G., "Development of Composite Ionizer Materials," Technical Report NASA CR-54188, April 1965.
5. Todd, H., Private Communication, June 1966.
6. Neal, R., Private Communication, June 1966.
7. Collins, R. E., "Flow of Fluids Through Porous Materials," Reinhold Pub. Corp., New York, N. Y., 1961.
8. Kuczynski, G. C., "Theory of Solid State Sintering," Powder Metallurgy, W. Leszynski, Ed. Interscience Publishers, New York, N. Y. 1961.
9. Ibid
10. Jones, W. D., "Fundamental Principles of Powder Metallurgy," Edward Arnold Publishers, Ltd., London, 1960.
11. Turk, R. R., Private Communication, June 1966.
12. Powell, R. A., "Isostatic Compaction of Metal Powders in Conventional Molding Tools," J. Powder Metallurgy, Vol. I, No. 3, pp 13-18, July 1965.
13. LaChance, M., Kuskevics, G., and Thompson, B., "High-Performance Cesium Ionizers Made from Sized Spherical Tungsten Powder," Presented at AIAA Fourth Electric Propulsion Conference, August 1964, AIAA Paper No. 64-592.
14. Husmann, O. K. and Turk, R., "Characteristics of Porous Tungsten Ionizers," presented at AIAA Fourth Electric Propulsion Conference, August 1964, AIAA Paper No. 64-691.
15. Forbes, S. G., "Development of a Modular Source Contact Ion Engine," Final Report AFAPL-TR-64-126, November 1964.
16. Kirkpatrick, M. E. and Mendelson, R. A., "Metallurgical Development of Porous Structures for Ion Engine Applications," Presented at AIAA Fifth Electric Propulsion Conference, March 1966.

Unclassified

Security Classification

DOCUMENT CONTROL DATA - R&D		
<i>(Security classification of title, body of abstract and indexing annotation must be entered when the overall report is classified)</i>		
1. ORIGINATING ACTIVITY (Corporate author) TRW Systems One Space Park Redondo Beach, California 90278		2a. REPORT SECURITY CLASSIFICATION Unclassified
		2b. GROUP
3. REPORT TITLE Final Report on the Development of High Performance Porous Tungsten Ionizers		
4. DESCRIPTIVE NOTES (Type of report and inclusive dates) March 1966 through November 1966		
5. AUTHOR(S) (Last name, first name, initial) Kirkpatrick, M. E. Mendelson, R. A.		
6. REPORT DATE January 1967	7a. TOTAL NO. OF PAGES 75	7b. NO. OF REFS 16
8a. CONTRACT OR GRANT NO. AF 33(615)-3817 ✓ b. PROJECT NO. 9-188 c. d.	9a. ORIGINATOR'S REPORT NUMBER(S) AFML-TR-67-21 ✓ 9b. OTHER REPORT NO(S) (Any other numbers that may be assigned this report) 05823-6005-R000 ✓	
10. AVAILABILITY/LIMITATION NOTICES DDC release to CFSTI is <u>NOT</u> authorized.		
11. SUPPLEMENTARY NOTES	12. SPONSORING MILITARY ACTIVITY Metallurgical Processing Branch Air Force Materials Laboratory Wright-Patterson AFB, Ohio 45433	
13. ABSTRACT <p>A development program directed toward the further development of techniques involved in the preparation and testing of porous tungsten ionizer materials is described. A current state-of-the-art survey is included to establish the status of porous ionizer material technology.</p> <p>Experimental results relating to particle size distribution and to the pore parameters of the resulting compacts are presented. Parameters such as sintering time and temperature, density, porosity, permeability, thermal stability, and ionizer performance were studied. The results to all the experimental investigations along with a description of the experimental approach are presented in this report.</p>		

DD FORM 1473
1 JAN 64

Unclassified
Security Classification

14. KEY WORDS	LINK A		LINK B		LINK C	
	ROLE	WT	ROLE	WT	ROLE	WT
Powder Metallurgy Tungsten Porous Bodies Contact Ionizers						

INSTRUCTIONS

1. **ORIGINATING ACTIVITY:** Enter the name and address of the contractor, subcontractor, grantee, Department of Defense activity or other organization (*corporate author*) issuing the report.
- 2a. **REPORT SECURITY CLASSIFICATION:** Enter the overall security classification of the report. Indicate whether "Restricted Data" is included. Marking is to be in accordance with appropriate security regulations.
- 2b. **GROUP:** Automatic downgrading is specified in DoD Directive 5200.10 and Armed Forces Industrial Manual. Enter the group number. Also, when applicable, show that optional markings have been used for Group 3 and Group 4 as authorized.
3. **REPORT TITLE:** Enter the complete report title in all capital letters. Titles in all cases should be unclassified. If a meaningful title cannot be selected without classification, show title classification in all capitals in parenthesis immediately following the title.
4. **DESCRIPTIVE NOTES:** If appropriate, enter the type of report, e.g., interim, progress, summary, annual, or final. Give the inclusive dates when a specific reporting period is covered.
5. **AUTHOR(S):** Enter the name(s) of author(s) as shown on or in the report. Enter last name, first name, middle initial. If military, show rank and branch of service. The name of the principal author is an absolute minimum requirement.
6. **REPORT DATE:** Enter the date of the report as day, month, year, or month, year. If more than one date appears on the report, use date of publication.
- 7a. **TOTAL NUMBER OF PAGES:** The total page count should follow normal pagination procedures, i.e., enter the number of pages containing information.
- 7b. **NUMBER OF REFERENCES:** Enter the total number of references cited in the report.
- 8a. **CONTRACT OR GRANT NUMBER:** If appropriate, enter the applicable number of the contract or grant under which the report was written.
- 8b, 8c, & 8d. **PROJECT NUMBER:** Enter the appropriate military department identification, such as project number, subproject number, system numbers, task number, etc.
- 9a. **ORIGINATOR'S REPORT NUMBER(S):** Enter the official report number by which the document will be identified and controlled by the originating activity. This number must be unique to this report.
- 9b. **OTHER REPORT NUMBER(S):** If the report has been assigned any other report numbers (*either by the originator or by the sponsor*), also enter this number(s).
10. **AVAILABILITY/LIMITATION NOTICES:** Enter any limitations on further dissemination of the report, other than those

imposed by security classification, using standard statements such as:

- (1) "Qualified requesters may obtain copies of this report from DDC."
- (2) "Foreign announcement and dissemination of this report by DDC is not authorized."
- (3) "U. S. Government agencies may obtain copies of this report directly from DDC. Other qualified DDC users shall request through _____."
- (4) "U. S. military agencies may obtain copies of this report directly from DDC. Other qualified users shall request through _____."
- (5) "All distribution of this report is controlled. Qualified DDC users shall request through _____."

If the report has been furnished to the Office of Technical Services, Department of Commerce, for sale to the public, indicate this fact and enter the price, if known.

11. **SUPPLEMENTARY NOTES:** Use for additional explanatory notes.
12. **SPONSORING MILITARY ACTIVITY:** Enter the name of the departmental project office or laboratory sponsoring (*paying for*) the research and development. Include address.
13. **ABSTRACT:** Enter an abstract giving a brief and factual summary of the document indicative of the report, even though it may also appear elsewhere in the body of the technical report. If additional space is required, a continuation sheet shall be attached.

It is highly desirable that the abstract of classified reports be unclassified. Each paragraph of the abstract shall end with an indication of the military security classification of the information in the paragraph, represented as (TS), (S), (C), or (U).

There is no limitation on the length of the abstract. However, the suggested length is from 150 to 225 words.

14. **KEY WORDS:** Key words are technically meaningful terms or short phrases that characterize a report and may be used as index entries for cataloging the report. Key words must be selected so that no security classification is required. Identifiers, such as equipment model designation, trade name, military project code name, geographic location, may be used as key words but will be followed by an indication of technical context. The assignment of links, rules, and weights is optional.

DEPARTMENT OF THE AIR FORCE
AIR FORCE MATERIALS LABORATORY: RTD (AFSC)
WRIGHT-PATTERSON AIR FORCE BASE, OHIO 45433



REPLY TO
ATTN OF: MATB (Mr. Gegel)

SUBJECT: Manufacturing Methods Final Technical Report Distribution, Project 9-188,
Report Nr. AFML-TR-67-21, Project Title: Development of Porous Tungsten
Ion Emitter Processing

TO:

1. Attached is a Final Technical Report for your information and use in your operation. Please acknowledge receipt by checking the appropriate item below.

- Require reports in this specific area.
 Do Not require reports in this specific area.
 Report addressed properly
 Improper address. Proper address is exactly as follows:

(Attn Line should be Department or Code, Not Person)

Company _____
Attn: _____
Street _____
City _____ State _____

2. Please return to:

AFML (MATB/Mr. G. A. Gegel)
Wright-Patterson AFB, Ohio 45433

A handwritten signature in cursive script, reading "H. A. Johnson", is written over the typed name.

H. A. JOHNSON
Chief, Metallurgical Processing Branch
Manufacturing Technology Division